Search for Higgs boson pair production in the $b\bar{b}\tau^{+}\tau^{-}$ final state with ATLAS

Cen Mo on behalf of the ATLAS Collaboration

Shanghai Jiao Tong University

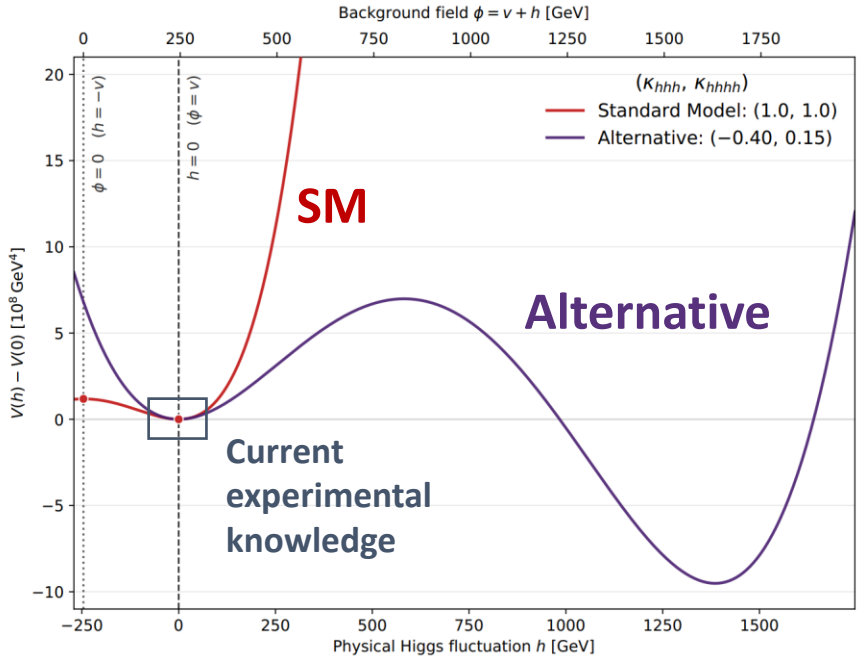
31 October, 2026

Search for Higgs Boson Pair Production

- **Higgs boson pair production (HH)** provides a direct probe of the trilinear Higgs boson self-coupling.

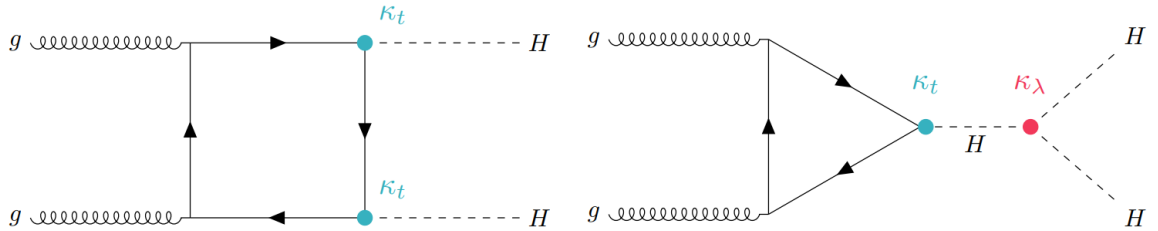
$$V(h) = \frac{1}{2}m_H^2 h^2 + \lambda_{hhh} v h^3 + \frac{1}{4}\lambda_{hhhh} h^4$$

- Search for HH and measure $\kappa_\lambda = \lambda_{hhh} \,/\, \lambda_{hhh}^{\mathrm{SM}}$ to probe the shape of Higgs potential:
  - Deviations from SM predictions could signal new Higgs-sector interactions, with implications for vacuum stability.

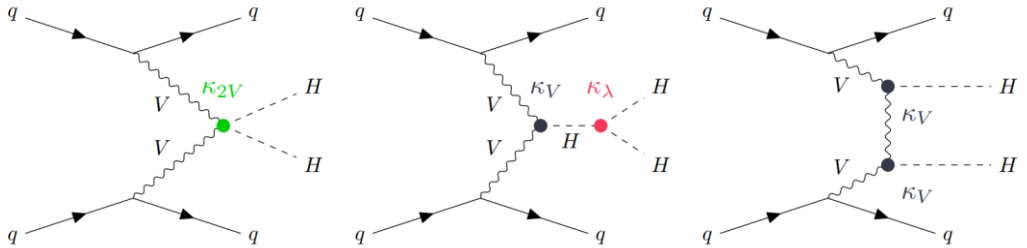


- Main production modes: ggF+VBF

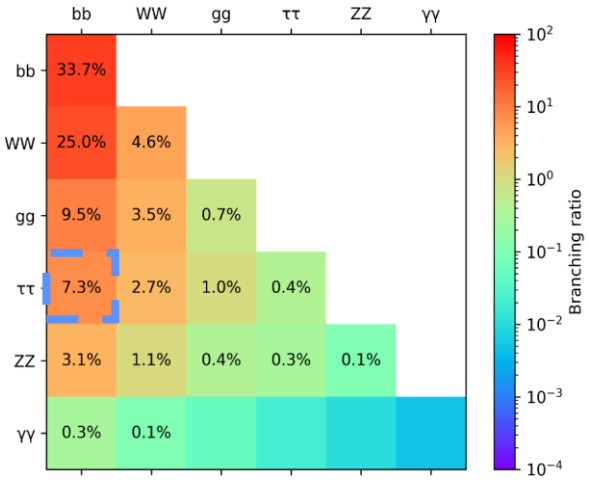
ggF: $\sigma_{13\ \mathrm{TeV}} \approx 31$ fb, $\sigma_{13.6\ \mathrm{TeV}} \approx 34$ fb



VBF: $\sigma_{13\ \mathrm{TeV}} \approx 1.7$ fb, $\sigma_{13.6\ \mathrm{TeV}} \approx 1.9$ fb



Search for $HH \to b\bar{b}\tau^+\tau^-$

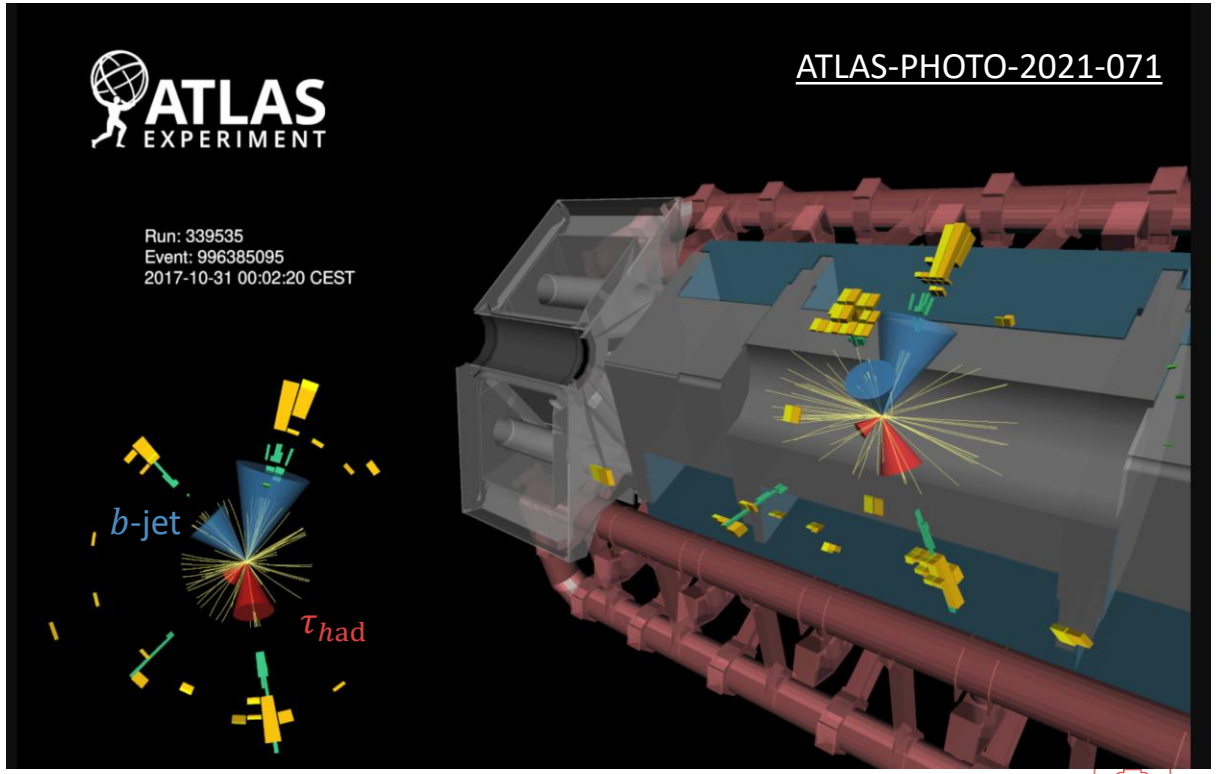


This is one of the most sensitive channels for HH searches:

- Good balance between purity (τ-leptons) and expected signal yield (BR$\sim$7.3%).

This search aims to:

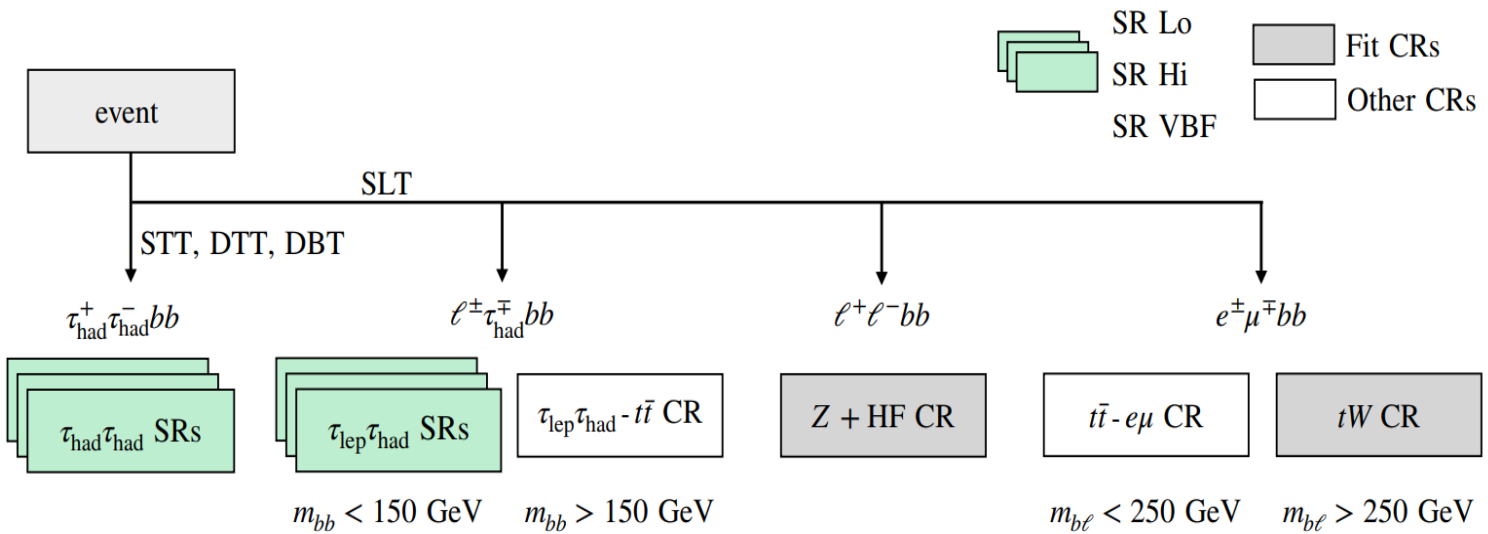
- Use Run 2 (140 fb^{-1}) + partial Run 3 (56 fb^{-1}) ATLAS data
- Focus on the $b\bar{b}\tau_{\mathrm{had}}\tau_{\mathrm{had}}$ and $b\bar{b}\tau_{\mathrm{lep}}\tau_{\mathrm{had}}$ channels
- Measure the following physics parameters:
  - HH production signal strength: μ_{HH}
  - Coupling modifiers: κ_λ, κ_{2V}
  - Signal strengths by production mode: μ_{ggF}, μ_{VBF}
  - Signal strengths for ZH and ZZ in the $b\bar{b}\tau^+\tau^-$ final state (validation measurement)



Event selections and region definitions

Electrons	Muons	*b*-Jets	τ_{had}
TightLH ID	Medium ID	GN2 tagger @ 85% WP	loose RNN ID

All regions shown here require exactly **2 b-jets** and an **oppositely charged** $\tau_{had}\tau_{had}$ / $l\tau_{had}$ / ll pair.



$$m_{bl} = \min[\max(m_{11}, m_{22}), \max(m_{12}, m_{21})]$$

Purpose of the CRs

- **$t\bar{t}$-$e\mu$ CR**: derive correction factors to improve $t\bar{t}$ modelling.
- **$\tau_{lep}\tau_{had}$-$t\bar{t}$ CR**: estimate $t\bar{t}$ with fake-τ_{had}
- **Z+HF CR**: derive norm factors (NFs) for the Z+hf and $t\bar{t}$ processes
- ***tW* CR**: derive NF for the *tW* process, constrain the $t\bar{t}$-tW interference shape uncertainty

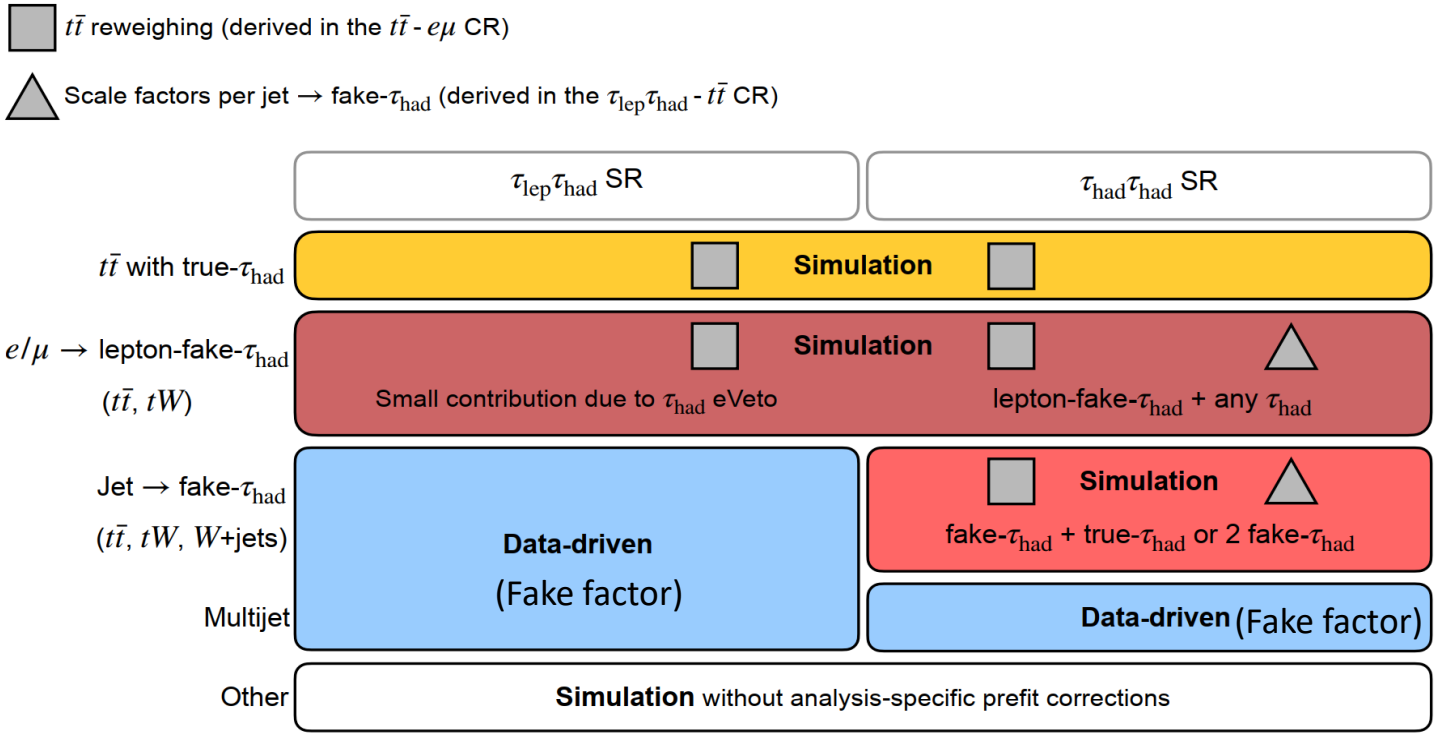
Triggers

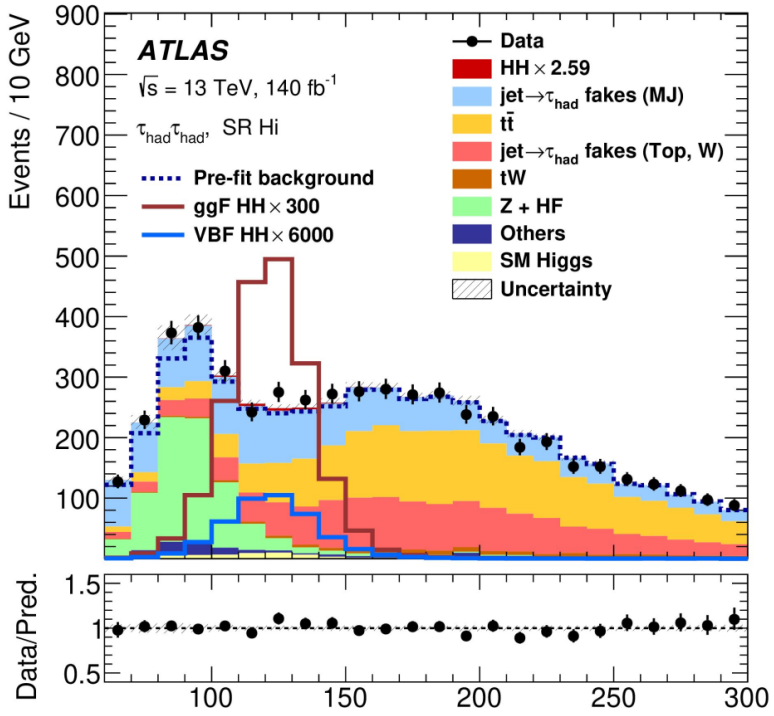
- $\tau_{had}\tau_{had}$: single-tau trigger (STT), di-tau trigger (DTT) and di-*b* trigger (DBT)
- $\tau_{lep}\tau_{had}$: single-lepton trigger (SLT)

Modelling of the main backgrounds

SM backgrounds that can mimic the $bb\tau\tau$ final state:

- **Z+heavy flavour (Z+HF), single Higgs, diboson**: modelled by MC.
- **$t\bar{t}$, tW, multijet with jet faking τ_{had}**: corrected by SFs, or estimated by data-driven methods before fitting.

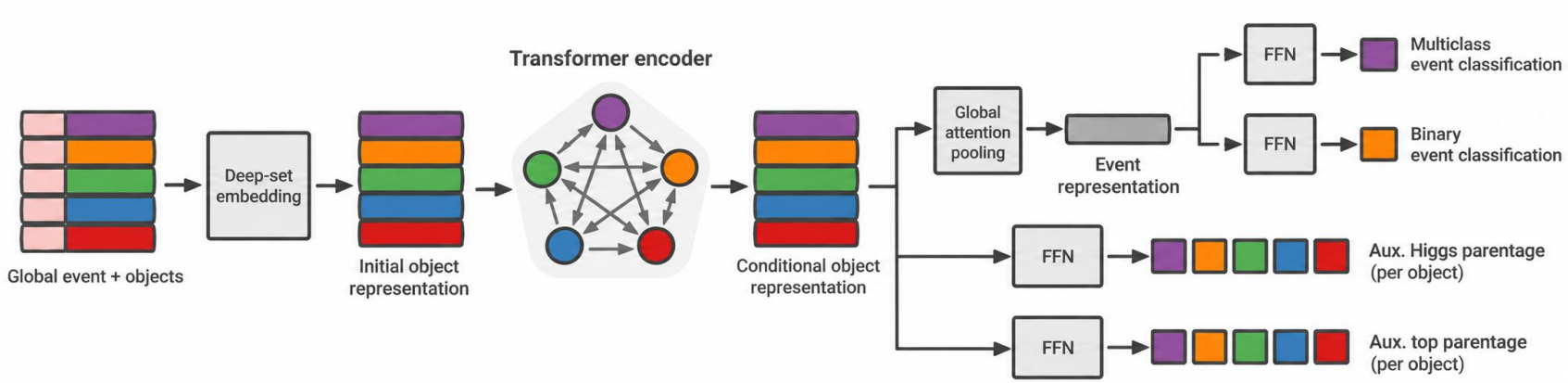




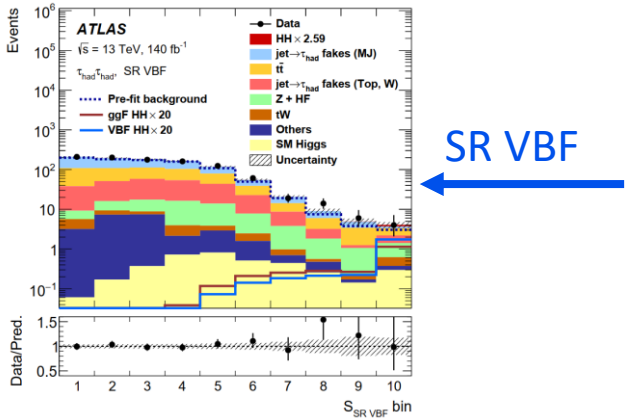
$\tau_{had}\tau_{had}$ SR: multiplicity and charge correlation of Jet→fake-τ_{had} are different in top and multijet samples, so different methods are used to estimate them.

Transformer-based multivariate analysis

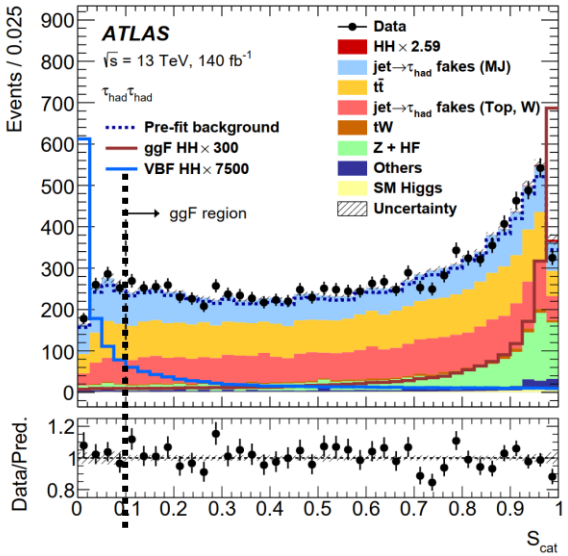
- A transformer-based classifier is trained for each channel to define fit observables.



- MVA scores are also used to define signal regions and observables for final fit.

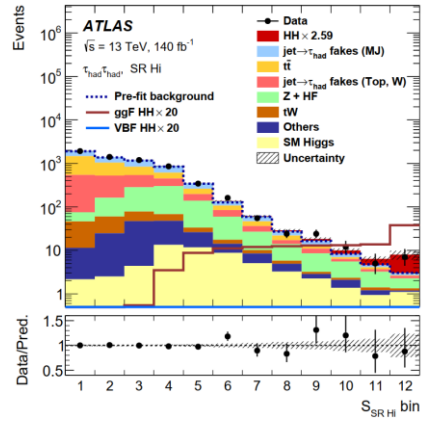


SR VBF

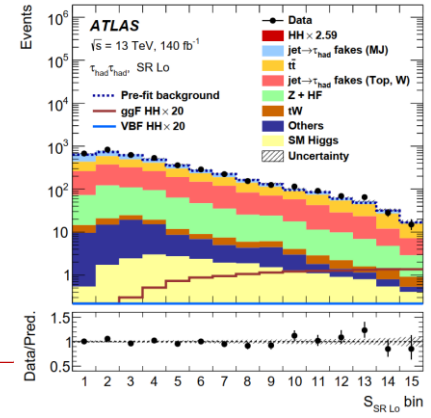


SR ggF

$m_{HH} > 350$ GeV: **SR hi**



$m_{HH} < 350$ GeV & main-stream: **SR lo**



Transformer inputs

- Objects: 2 b-jets, 2 τ(hadronic or leptonic), MET, MMC, 3 light flavour jets

Object-level features

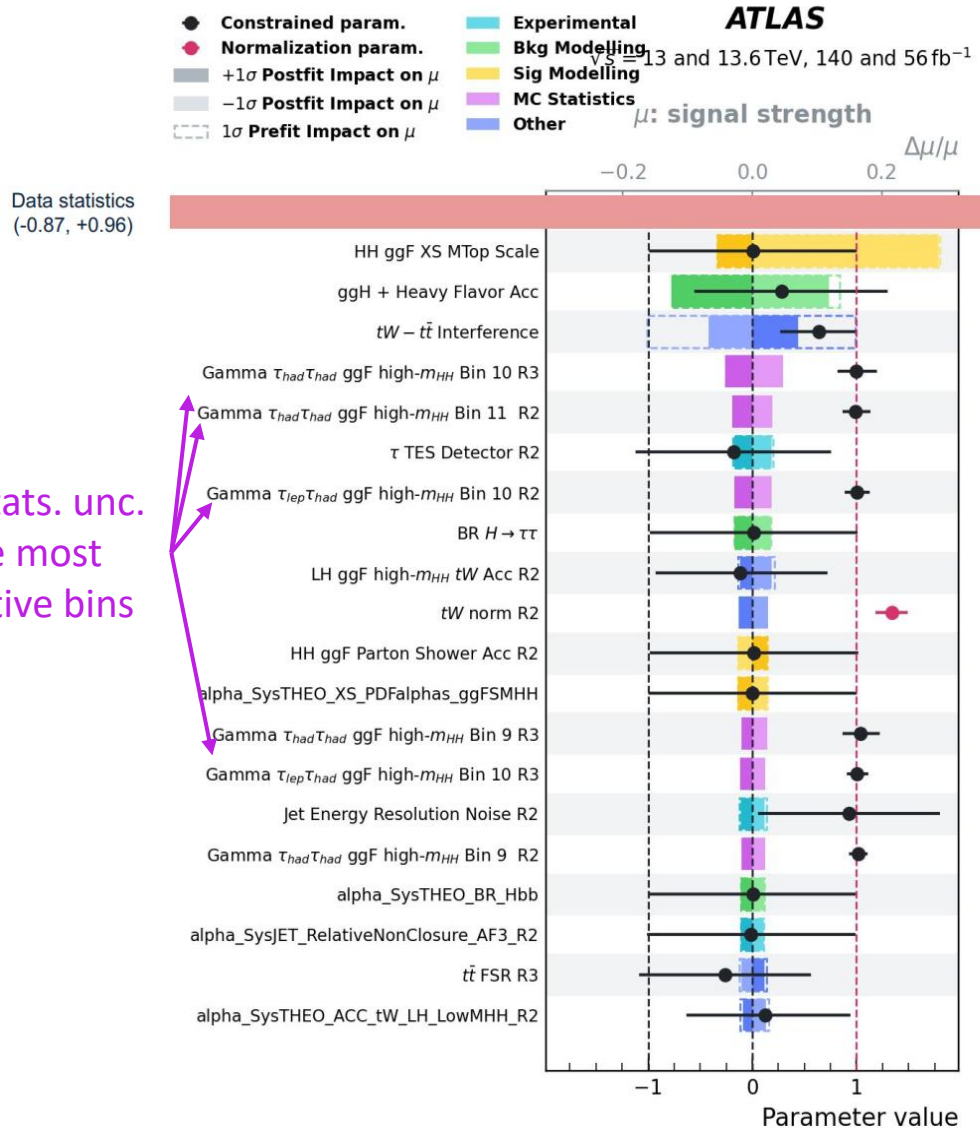
Object-level features (per-object inputs to the transformer network)	
η	Pseudorapidity; set to 0 for $\vec{p}_{\mathrm{T}}^{\,\mathrm{miss}}$
ϕ	Azimuthal angle
m	Mass; set to 0 for $\vec{p}_{\mathrm{T}}^{\,\mathrm{miss}}$, leptons, and τ_{had} candidates
p_{T}	Transverse momentum
PCBT	GN2 pseudo-continuous b-tagging score (bins: 100%–90%–85%–77%–70%–65%) set to -2 for non-jet objects and -1 for forward jets
isTau	Boolean flag: object is a τ_{had} candidate
isJet	Boolean flag: object is a non-b-tagged jet
isBjet	Boolean flag: object is a b-tagged jet
isMET	Boolean flag: object is $\vec{p}_{\mathrm{T}}^{\,\mathrm{miss}}$
isMMC	Boolean flag: object is the MMC di-τ system
isLepton	Boolean flag: object is a lepton (only in $\tau_{\mathrm{lep}}\tau_{\mathrm{had}}$ channel)

Event-level features

Variable	Description	
	Global event-level features: both channels	
m_{HH}	Invariant mass of the reconstructed HH system using the di-τ four-momentum after the MMC algorithm	Common
m_{bb}	Invariant mass of the b-jet pair	Common
ΔR_{bb}	ΔR between the two b-jets	Common
m_{jj}	Invariant mass of the two leading VBF jets	Common
ΔR_{jj}	ΔR between the two leading VBF jets	Common
$\eta_{\mathrm{VBF}\ j_0} \cdot \eta_{\mathrm{VBF}\ j_1}$	Product of pseudorapidities of the two leading VBF jets	Common
	Global event-level features: $\tau_{\mathrm{had}}\tau_{\mathrm{had}}$ only	
$\Delta R_{\tau\tau}$	ΔR between the two τ_{had} candidates	HadHad-only
	Global event-level features: $\tau_{\mathrm{lep}}\tau_{\mathrm{had}}$ only	
$\Delta R(\tau_{\mathrm{had}}, \ell)$	ΔR between the τ_{had} candidate and the electron or muon	LepHad-only
$p_{\mathrm{T},HH}$	Transverse momentum of the reconstructed HH system	LepHad-only
η_{HH}	Pseudorapidity of the reconstructed HH system	LepHad-only
$E_{\mathrm{T}}^{\mathrm{miss}}$	Missing transverse energy	LepHad-only
$\Delta R(b_0, \tau_{\mathrm{had}})$	ΔR between the leading b-jet and the τ_{had} candidate	LepHad-only
$\Delta R(b_1, \tau_{\mathrm{had}})$	ΔR between the subleading b-jet and the τ_{had} candidate	LepHad-only
$m_{b\ell}$	$\min(x, y)$, where $x = \max(m_{b_1,\tau_{\mathrm{had}}}, m_{b_2,\ell})$ and $y = \max(m_{b_1,\ell}, m_{b_2,\tau_{\mathrm{had}}})$	LepHad-only
$m_{\tau\tau}^{\mathrm{vis}}$	Invariant mass of the visible di-τ system	LepHad-only
$p_{\mathrm{T},\tau\tau}^{\mathrm{vis}}$	Transverse momentum of the visible di-τ system	LepHad-only
T_1	Topness [116], with $\sigma_t = \sigma_W = 5$ GeV	LepHad-only
H_{T}	Scalar sum of transverse momenta of all reconstructed objects	LepHad-only
$\Delta\eta(bb, \tau\tau)$	$\Delta\eta$ between the b-jet pair and the MMC di-τ systems	LepHad-only
$\Delta\phi(\tau\tau, E_{\mathrm{T}}^{\mathrm{miss}})$	$\Delta\phi$ between $\vec{p}_{\mathrm{T}}^{\,\mathrm{miss}}$ and the MMC di-τ system	LepHad-only
$\Delta R(b_1, \ell)$	ΔR between the subleading b-jet and the lepton	LepHad-only
$m_{\mathrm{T}}(\tau_{\mathrm{had}}, \vec{p}_{\mathrm{T}}^{\,\mathrm{miss}})$	Transverse mass of the τ_{had} candidate and $\vec{p}_{\mathrm{T}}^{\,\mathrm{miss}}$ system	LepHad-only

The upgraded MVA brings 20% improvements compared to the previous BDT-based method.

Impact of systematics



MC stats. unc. of the most sensitive bins

Ranked by impact:

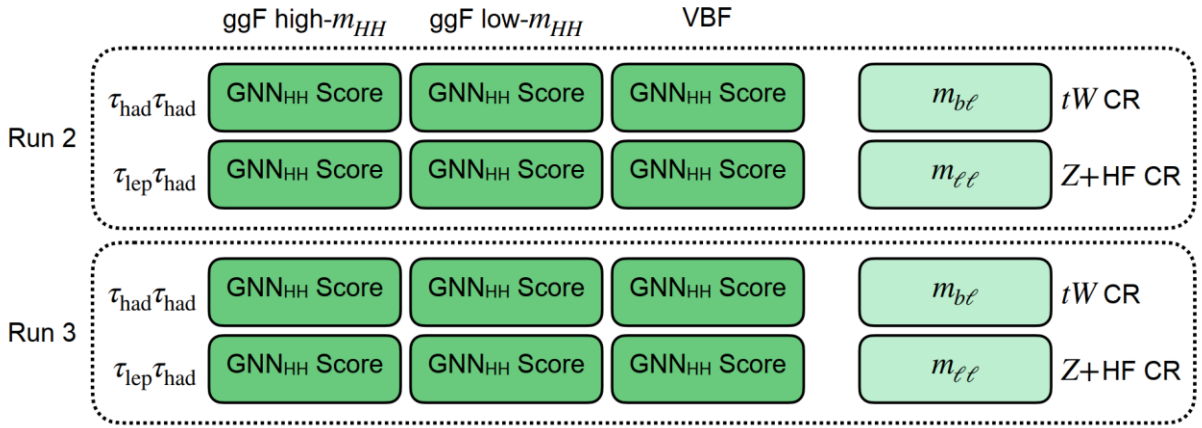
- Data statistical uncertainty **has the dominant impact.**

Leading systematic uncertainty

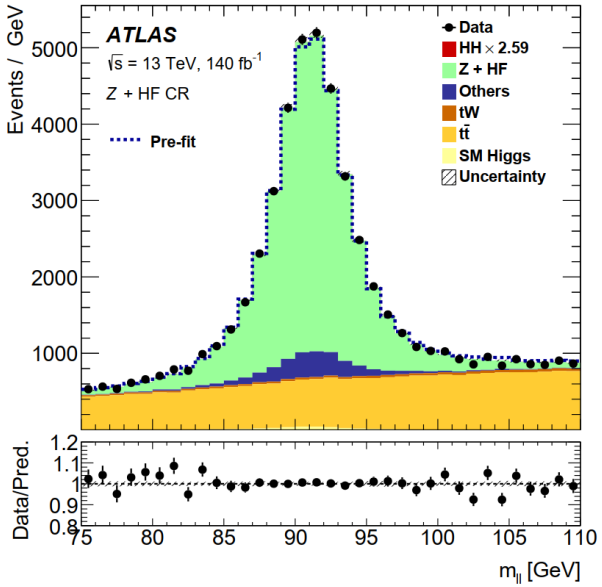
- Among **systematic uncertainties**, the **cross-section uncertainty on the ggF *HH* signal** has the largest impact.
- Among **background modelling** uncertainties, the **acceptance unc. for ggH + heavy flavour** (with prior=100%) shows the largest impact.
- The *tW* CR tightly constrains the **tW-$t\bar{t}$ interference shape uncertainty**.

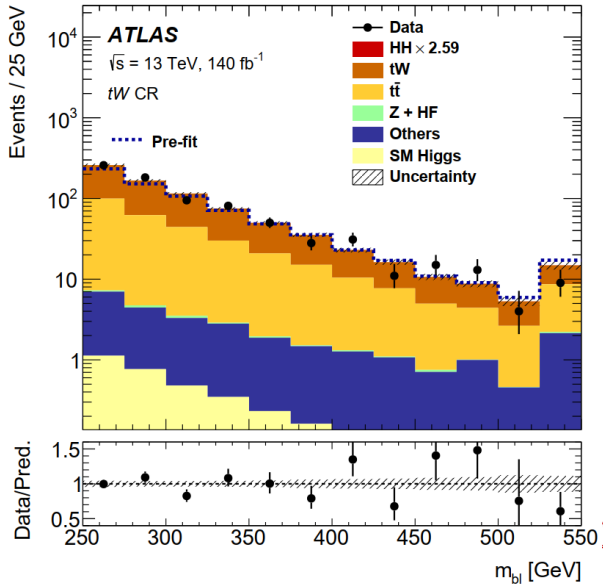
Statistical inference

- Binned profile-likelihood fit to extract POIs



- Z+HF CR and tW CR are designed to constrain the normalizations of Z+HF, $t\bar{t}$, and tW





Results

Results - HH signal strength

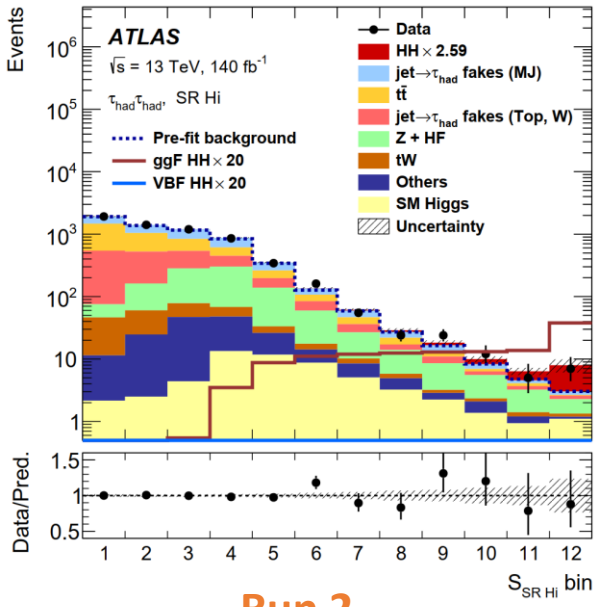
$$\mu_{HH} = 2.6^{+1.4}_{-1.0} = 2.59^{+1.0}_{-0.9}(\text{stat.})^{+1.0}_{-0.5}(\text{syst.})$$

Observed (expected) **significance**: 2.6 (1.2)σ

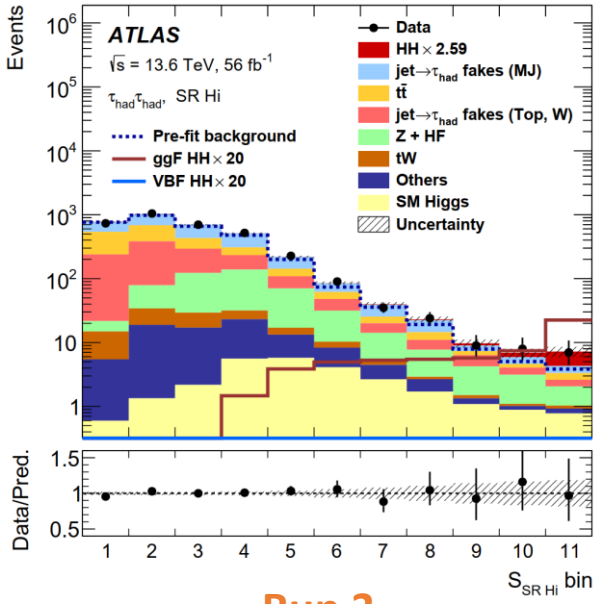
Observed (expected) **95% CL upper limit**: 5.3 (2.4 for the background-only hypothesis)

Compatible with SM prediction at 1.7 standard deviation

HadHad channel

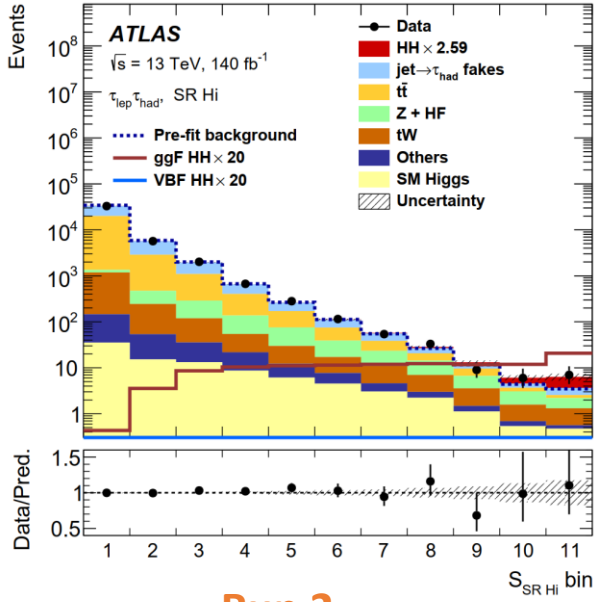


Run 2

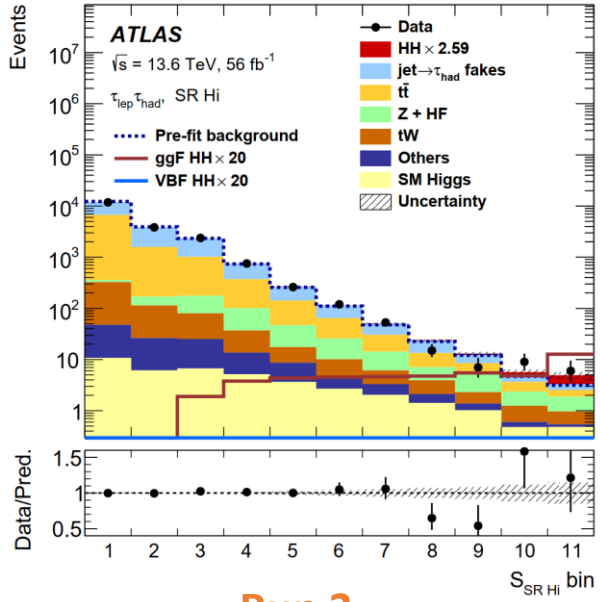


Run 3

LepHad channel



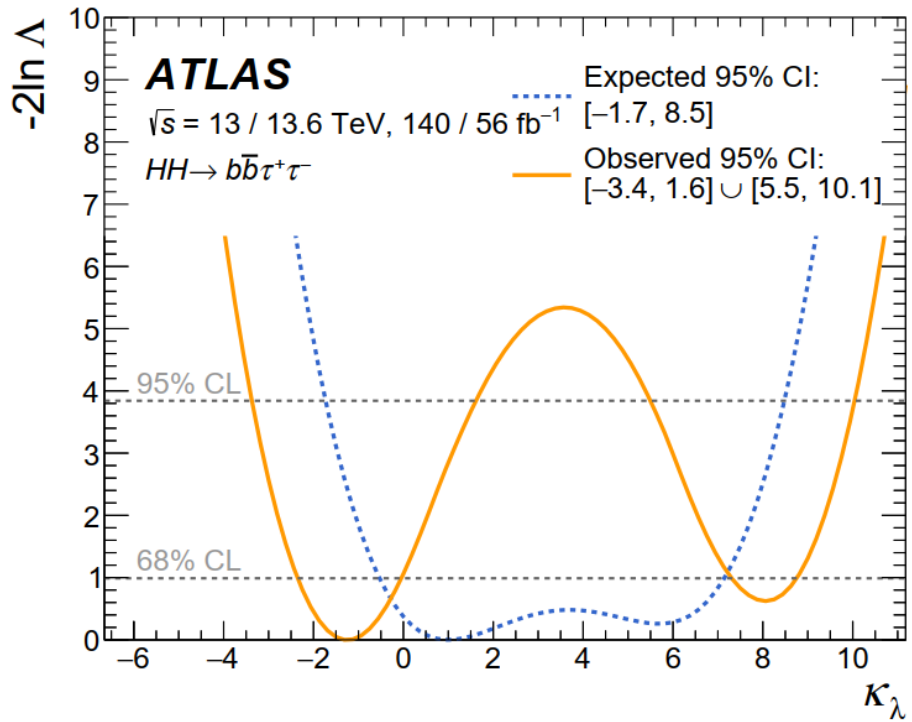
Run 2



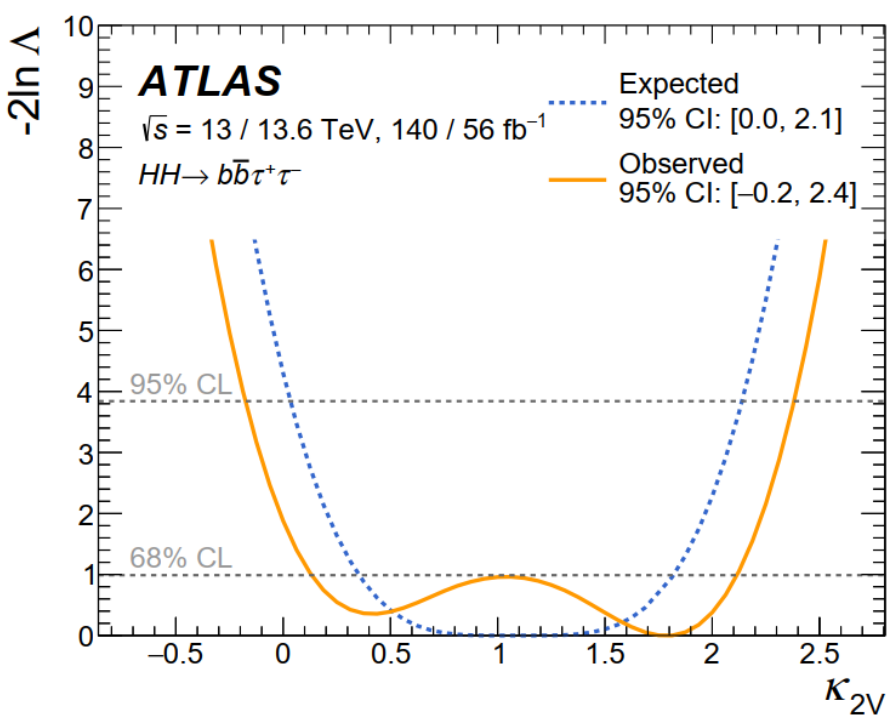
Run 3

Results - κ_λ and κ_{2V}

κ_λ (fix κ_{2V}=1)



κ_{2V} (fix κ_λ=1)

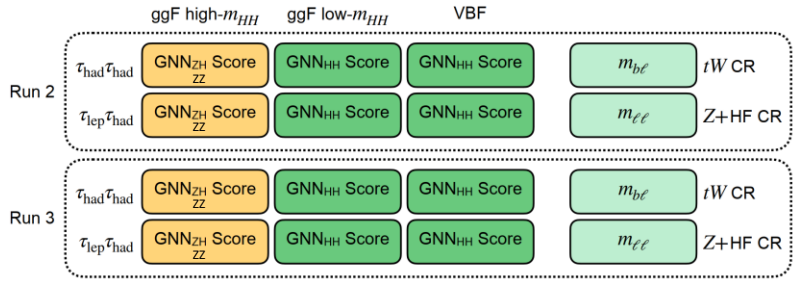


A degeneracy arises because different κ values can yield similar $\sigma \times A \times \epsilon$ due to interference terms between triangle and box amplitudes.

κ_λ	Expected	Observed
68% CI	[-0.52, 7.15]	[-2.34, -0.04] & [7.31, 8.76]
95% CI	**[-1.73, 8.49]**	**[-3.37, 1.61] & [5.51, 10.06]**

κ_{2V}	Expected	Observed
68% CI	[0.36, 1.83]	[0.14, 2.12]
95% CI	**[0.04, 2.14]**	**[-0.17, 2.39]**

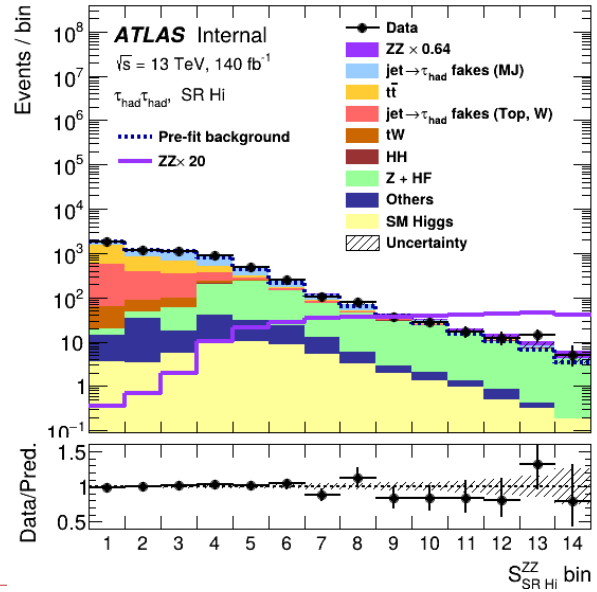
First evidence of ZH → $bb\tau\tau$ at ATLAS



- **ZZ/ZH→ $bb\tau\tau$ are used as standard candles to validate the $HH \to bb\tau\tau$ search.**
- They share the same analysis chain as the HH search, changing only the MVA score in the SR-hi to improve sensitivity to ZZ/ZH.
- Results are consistent with the SM.

$$\mu_{ZZ} = 0.64^{+0.39}_{-0.36}$$

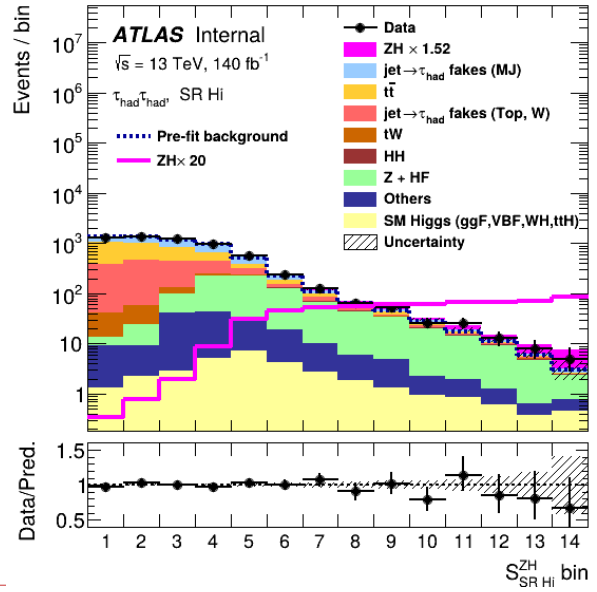
Observed (expected) **significance**: 1.83 (2.69)



First evidence for $ZH \to bb\tau\tau$

$$\mu_{ZH} = 1.52^{+0.52}_{-0.48}$$

Observed (expected) **significance**: 3.52 (2.42)



Summary

- We present results from a search for $HH \to b\bar{b}\tau^+\tau^-$ using Run 2 (140 fb^{-1}) + partial Run 3 (2022 + 2023, 56 fb^{-1}) data.

HH signal strength

$$\mu_{HH} = 2.6^{+1.4}_{-1.0} = 2.59^{+1.0}_{-0.9}(\text{stat.})^{+1.0}_{-0.5}(\text{syst.})$$

- The results on μ_{HH} show:
  - Observed (expected) **significance**: **2.6** (1.2)
  - Observed (expected) 95% CL upper **limit**: **5.3** (2.4 for μ_{HH}=0)
  - Compatible with SM at 1.7σ

- ZZ/ZH $\to bb\tau\tau$ measurements provides additional support for analysis strategy and background modelling:
  - **ZZ** signal: observed (expected) significance: 1.8 (2.7).
  - **ZH** signal: observed (expected) significance: **3.5** (2.4).
  - Both consistent with SM.

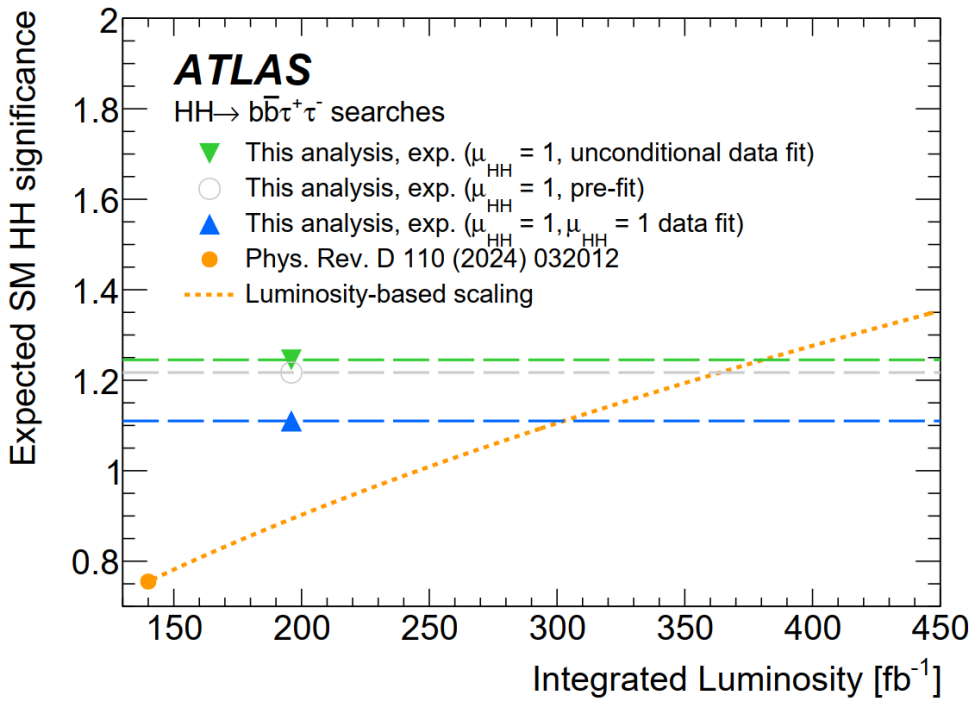
ZZ, ZH signal strengths

$$\mu_{ZZ} = 0.6^{+0.4}_{-0.4,} \qquad \mu_{ZH} = 1.5^{+0.5}_{-0.5}$$

First ZH $\to b\bar{b}\tau^+\tau^-$ Evidence!

65% improvement w.r.t. previous analysis

- More data, better b-jet ID and MVA strategy

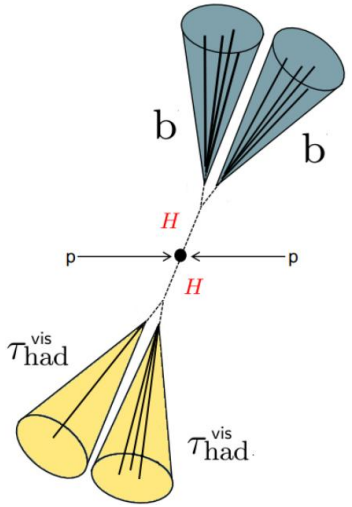


Backup

MC Sample list

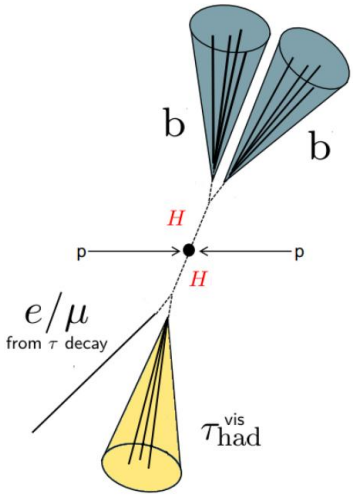
Process	ME generator	ME QCD order	PDF set	PS and hadronisation	UE model tune	Cross-section order
Signal						
$gg \to HH$ (ggF)	PowHeg Box v2 [65]	NLO	PDF4LHC21 [66]	Pythia 8.309 [67]	A14 [69] NNPDF2.3LO [68]	NNLO FTApprox
$qq \to qqHH$ (VBF)	MadGraph5_aMC@NLO 3.3.1 [70]	LO	NNPDF3.0NLO [71]	Pythia 8.308	A14 NNPDF2.3LO	N^3LO(QCD)+NLO(EW)
Top-quark						
$t\bar{t}$	PowHeg Box v2	NLO	NNPDF3.0NLO	Pythia 8.230 [75] [8.308]	A14 NNPDF2.3LO	NNLO+NNLL
Single top (t-chan.)	PowHeg Box v2	NLO	NNPDF3.0NLO	Pythia 8.230 [8.308]	A14 NNPDF2.3LO	NLO
Single top (s-chan.)	PowHeg Box v2	NLO	NNPDF3.0NLO	Pythia 8.230 [8.308]	A14 NNPDF2.3LO	NLO
Single top (tW)	PowHeg Box v2	NLO	NNPDF3.0NLO	Pythia 8.230 [8.308]	A14 NNPDF2.3LO	NLO
$t\bar{t}Z$	MadGraph5_aMC@NLO 2.8.1 [3.5.1]	NLO	NNPDF3.0NNLO	Pythia 8.244 [8.309]	A14 NNPDF2.3LO	NLO
$t\bar{t}W$	Sherpa 2.2.11 [Sherpa 2.2.14] [77]	NLO	NNPDF3.0NNLO	Sherpa 2.2.14	-	NLO
Vector boson + jets						
W+jets	Sherpa 2.2.11 [Sherpa 2.2.14]	NLO($\leq$ 2 jets) LO(3, 4, 5 jets)	NNPDF3.0NNLO	Sherpa 2.2.11 [Sherpa 2.2.14]	-	NNLO
Z+jets	Sherpa 2.2.14	NLO($\leq$ 2 jets) LO(3, 4, 5 jets)	NNPDF3.0NNLO	Sherpa 2.2.14	-	NNLO
Diboson						
WW, WZ, ZZ	Sherpa 2.2.14, Sherpa 2.2.16	NLO($\leq$ 1 jet) LO(2, 3 jets)	NNPDF3.0NNLO	Sherpa 2.2.14, Sherpa 2.2.16	-	NLO
Single Higgs boson						
ggF	PowHeg Box v2	NNLO	PDF4LHC15NNLO [87]	Pythia 8.212 [8.310]	AZNLO [89] [A14 NNPDF2.3LO]	N^3LO(QCD)+NLO(EW)
VBF	PowHeg Box v2	NLO	PDF4LHC15NLO	Pythia 8.230 [8.310]	AZNLO [A14 NNPDF2.3LO]	NNLO(QCD)+NLO(EW)
$qq \to WH$	PowHeg Box v2	NLO	NNPDF3.0NLO	Pythia 8.212,8.245 [8.309]	AZNLO [A14 NNPDF2.3LO]	NNLO(QCD)+NLO(EW)
$qq \to ZH$	PowHeg Box v2	NLO	NNPDF3.0NLO	Pythia 8.244,8.245 [8.309]	AZNLO [A14 NNPDF2.3LO]	NNLO(QCD)+NLO(EW)†
$gg \to ZH$	PowHeg Box v2	NLO	NNPDF3.0NLO	Pythia 8.307 [8.309]	AZNLO [A14 NNPDF2.3LO]	NLO+NLL
$t\bar{t}H$	PowHeg Box v2	NLO	NNPDF3.0NLO [PDF4LHC21]	Pythia 8.230 [8.308]	A14 NNPDF2.3LO	NLO(QCD)+NLO(EW)

Triggers & Object Selections



HadHad channel

- Targets the $\tau_{\mathrm{had}}\tau_{\mathrm{had}}$ final state.
- Triggered by single-/di-tau triggers or a $2b$+2j trigger
- Requires two b-jets and an oppositely charged τ_{had} pair



LepHad channel

- Targets the $\tau_{\mathrm{had}}\tau_{\mathrm{lep}}$ final state.
- Triggered by single-lepton triggers
- Requires 2 b-jets and oppositely charged τ_{had}+e/μ pair

Object selections

- $\boldsymbol{b}$**-jets**: GN2 flavour tagging at the 85% b-tagging efficiency working point.
- $\boldsymbol{\tau_{\mathrm{had}}}$: RNN-based ID algorithm at the loose working point.
  - $m_{\tau\tau}$ reconstructed using the Missing Mass Calculator to account for neutrinos.
- **Electron**: likelihood-based ID at tight working point.
- **Muon**: medium working point.

Trigger bucketing strategy

STT (Main-stream) *Lower cuts in 2015 and parts of 2016

DTT (Main-stream)

DTT (Delayed-stream)

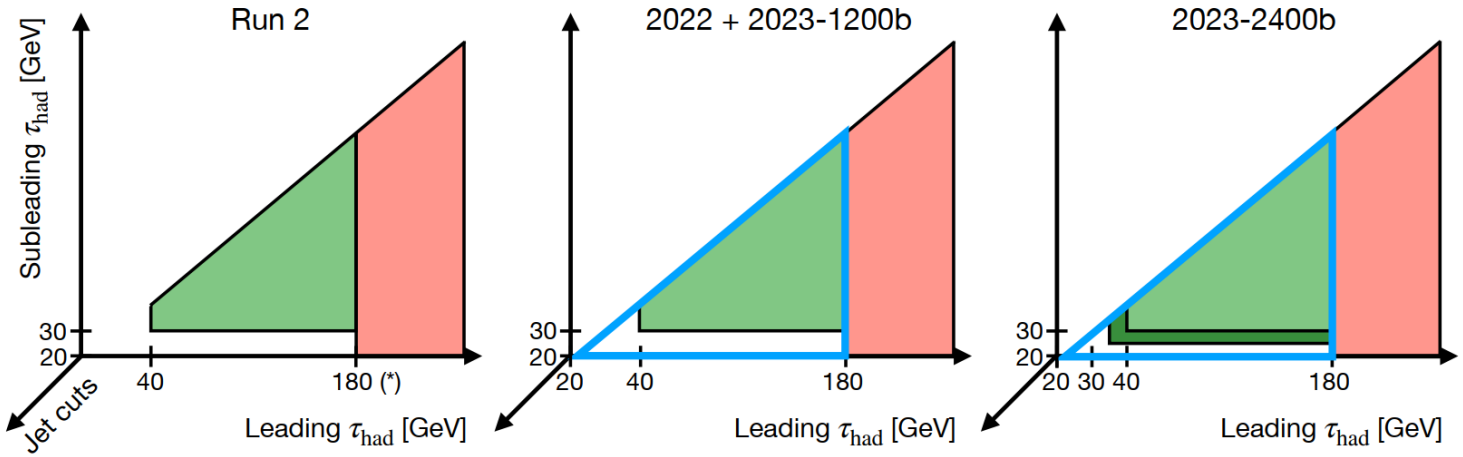
DBT (Delayed-stream) Orthogonal to STT and DTT buckets (jet p_T cuts)

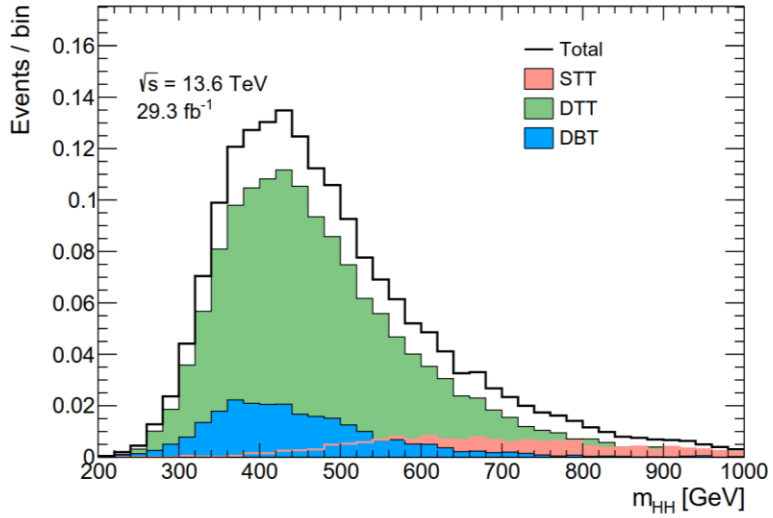
p_T-ordered array of jets and τ_{had}: p_T > [85, 60, 50, 25] GeV

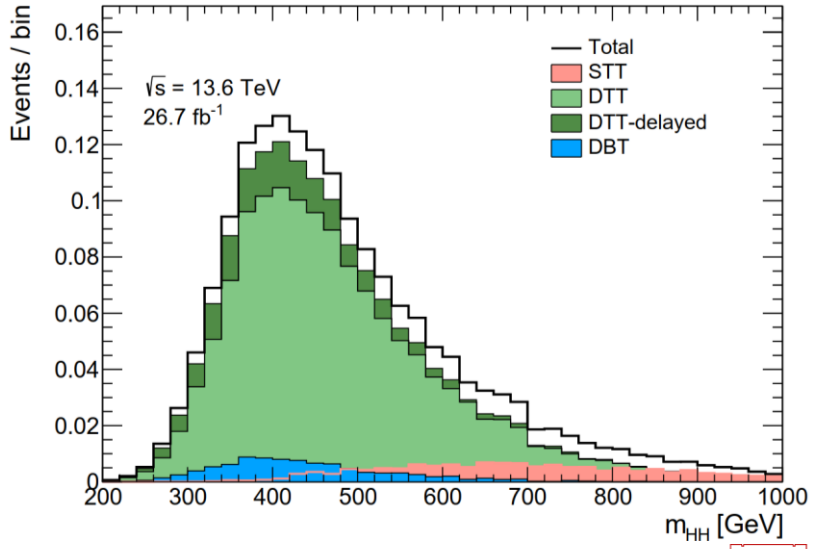
Bucket 1: Single-τ_{had} trigger (STT)

Bucket 2: Di-τ_{had} trigger (DTT)

Bucket 3: Di-b trigger (DBT)

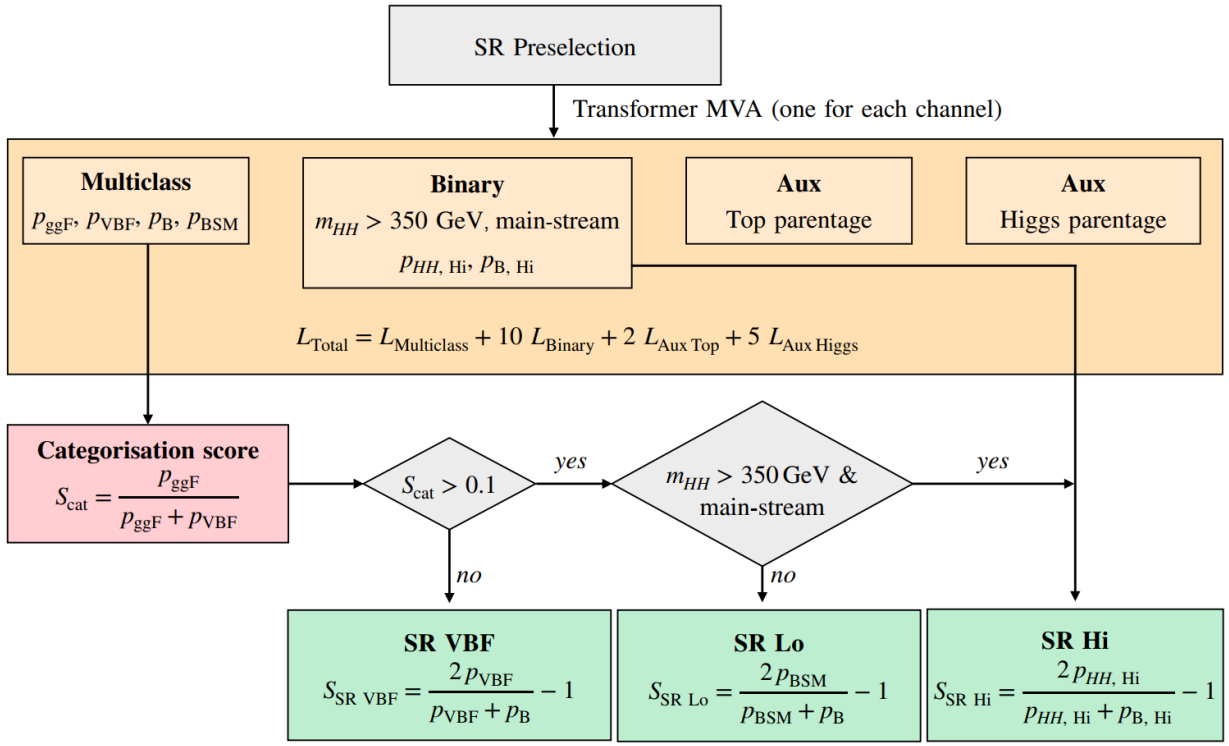






MVA strategy

- A graph-transformer-based neural network is used.
- **Trained two neural networks: one per channel**.
  For each channel, Run 2 and Run 3 share the same network.
- Five-fold cross-validation is used.
- **Robust model choice**: an ensemble of 20 models is trained; the model with validation performance closest to the ensemble mean is selected.
- Each network is trained with several tasks simultaneously:



Task	Multiclass	Binary	Aux
Trained to classify	ggF, VBF, κ_λ=5 (BSM) signal, background	Signal, background in high-m_{HH} region	Origin of particles (Higgs, top, others)
Usage in the analysis	Split inclusive SR into **three SRs***; discriminant for **VBF & low-m_{HH} SRs**	discriminant for **high-m_{HH} SR**	Not used

*Three SRs: VBF SR, ggF low-m_{HH} SR and ggF high-m_{HH} SR

Systematic uncertainties

Experimental Uncertainties

Source	Reduction scheme
EGamma	Simplified (EFF Reco in Run 2), Total (rest) reduction scheme (limited sensitivity)
Muon	Tightest reduction scheme (limited sensitivity)
Tau	Standard
FTAG	No reduction available, thus the full set of uncertainties is used
JES	Category-based reduction
JER	Full set of uncertainties is used

Signal Cross-section Uncertainties

ggF *HH*	(Scale and m_t)	(PDF + α_s)
Run 2	+6% -23%	±2.3%
Run 3	+6% -23%	±2.3%
VBF *HH*	Scale	(PDF + α_s)
Run 2	+0.05% -0.04%	±2.7%
Run 3	+0.05% -0.03%	±2.7%

Modelling Uncertainties

Uncertainties in cross section, parton showering, ISR, FSR …

- **Cross-section uncertainties.**
- **Relative acceptance uncertainties**: relative acceptance (relative to CR) variation (for $t\bar{t}$, *tW*, Z+hf processes)
- **Acceptance uncertainties**: acceptance variation (other processes)
- **Shape uncertainties** on fit discriminants

Other Sources of Uncertainties

- **Stat. uncertainties** of background template
- Uncertainties of **data-driven fake-τ_{had}** estimation
- Uncertainties of **$t\bar{t}$ reweighting**
- Uncertainty of **Z p_{T} non-closure** for Z+jets

Kappa parameterization

- Parameterization of ggF *HH*: κ_λ=(0, 1, 5) as basis

$$\text{sample}(\kappa_\lambda, \kappa_t) = \kappa_t \left[\left(\kappa_t^2 + \frac{\kappa_\lambda^2}{5} - \frac{6}{5}\kappa_\lambda\kappa_t \right) \text{sample}(0, 1) + \left(\frac{5}{4}\kappa_\lambda\kappa_t - \frac{\kappa_\lambda^2}{4} \right) \text{sample}(1, 1) + \left(\frac{\kappa_\lambda^2 - \kappa_\lambda\kappa_t}{20} \right) \text{sample}(5, 1) \right].$$

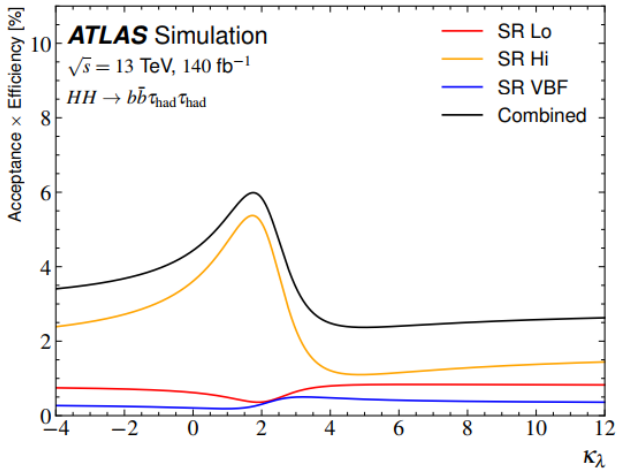
- Parameterization of VBF *HH*

basis

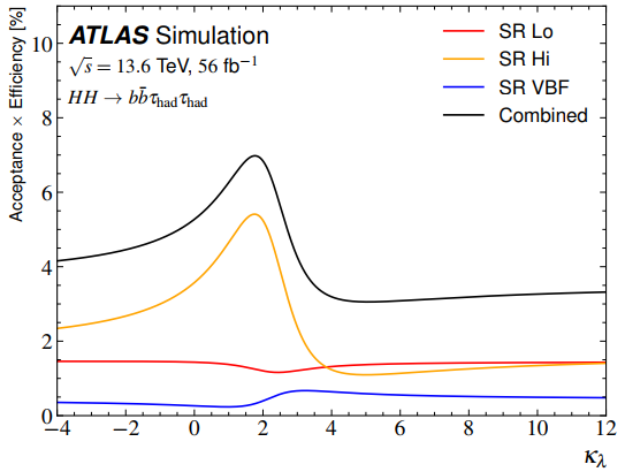
κ_λ	κ_{2V}	κ_V
1	1	1
-5	1	$\frac{1}{2}$
10	1	1
2	1	1
1	$\frac{3}{2}$	1
1	1	$\frac{1}{2}$

$$\begin{aligned}\text{sample}(\kappa_\lambda, \kappa_{2V}, \kappa_V) = &\left(\frac{\kappa_\lambda^2\kappa_V^2}{9} + \frac{68}{135}\kappa_{2V}^2 + \frac{772}{135}\kappa_V^4 + \frac{20}{27}\kappa_\lambda\kappa_{2V}\kappa_V - \frac{56}{27}\kappa_\lambda\kappa_V^3 - 4\kappa_{2V}\kappa_V^2 \right) \text{sample}(1, 1, 1) \\ &+ \left(\frac{8}{48}\kappa_{2V}^2 - \frac{8}{45}\kappa_V^4 - \frac{4}{9}\kappa_\lambda\kappa_{2V}\kappa_V + \frac{4}{9}\kappa_\lambda\kappa_V^3 \right) \text{sample}(-5, 1, \frac{1}{2}) \\ &+ \left(\frac{\kappa_\lambda^2\kappa_V^2}{72} - \frac{11}{540}\kappa_{2V}^2 + \frac{13}{270}\kappa_V^4 + \frac{11}{216}\kappa_\lambda\kappa_{2V}\kappa_V - \frac{5}{54}\kappa_\lambda\kappa_V^3 \right) \text{sample}(10, 1, 1) \\ &+ \left(\frac{11}{60}\kappa_{2V}^2 - \frac{\kappa_\lambda^2\kappa_V^2}{8} - \frac{53}{30}\kappa_V^4 - \frac{19}{24}\kappa_\lambda\kappa_{2V}\kappa_V + \frac{13}{6}\kappa_\lambda\kappa_V^3 + \frac{1}{3}\kappa_{2V}\kappa_V^2 \right) \text{sample}(2, 1, 1) \\ &+ \left(4\kappa_{2V}\kappa_V^2 - \frac{4}{5}\kappa_{2V}^2 - \frac{16}{5}\kappa_V^4 \right) \text{sample}(1, \frac{3}{2}, 1) \\ &+ \left(\frac{88}{45}\kappa_{2V}^2 + \frac{152}{45}\kappa_V^4 + \frac{4}{9}\kappa_\lambda\kappa_{2V}\kappa_V - \frac{4}{9}\kappa_\lambda\kappa_V^3 - \frac{16}{3}\kappa_{2V}\kappa_V^2 \right) \text{sample}(1, 1, \frac{1}{2}).\end{aligned} \tag{B.5}$$

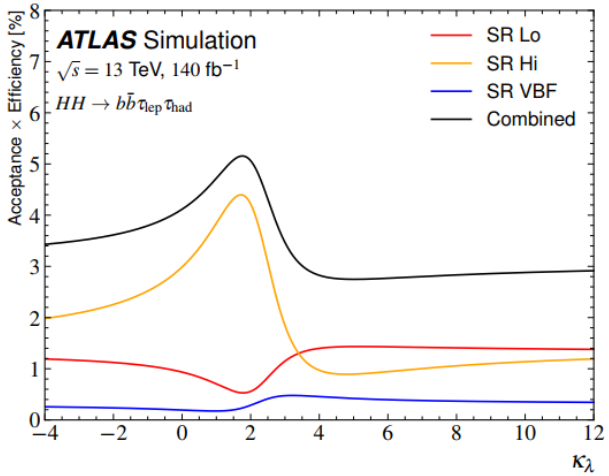
Acceptance vs. κ_λ



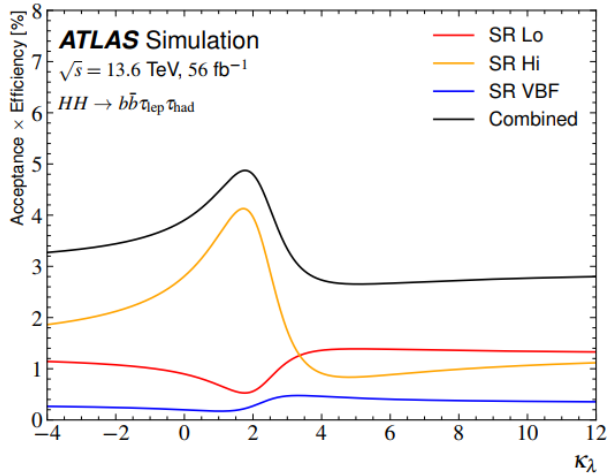
(a)



(b)

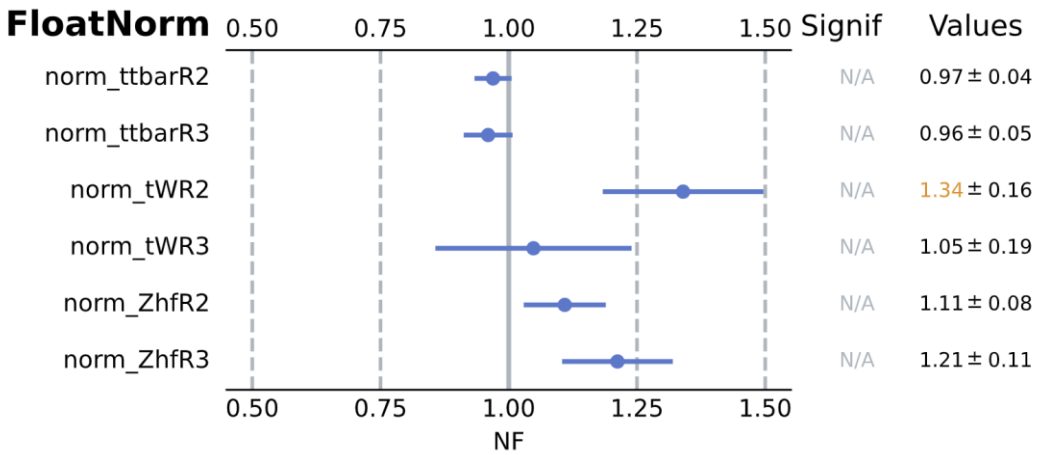


(c)

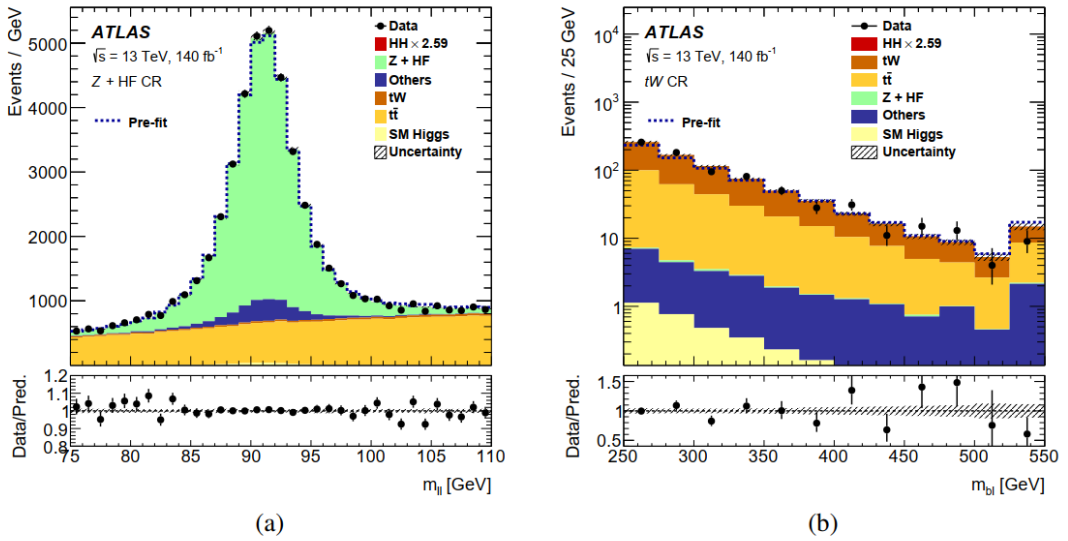


(d)

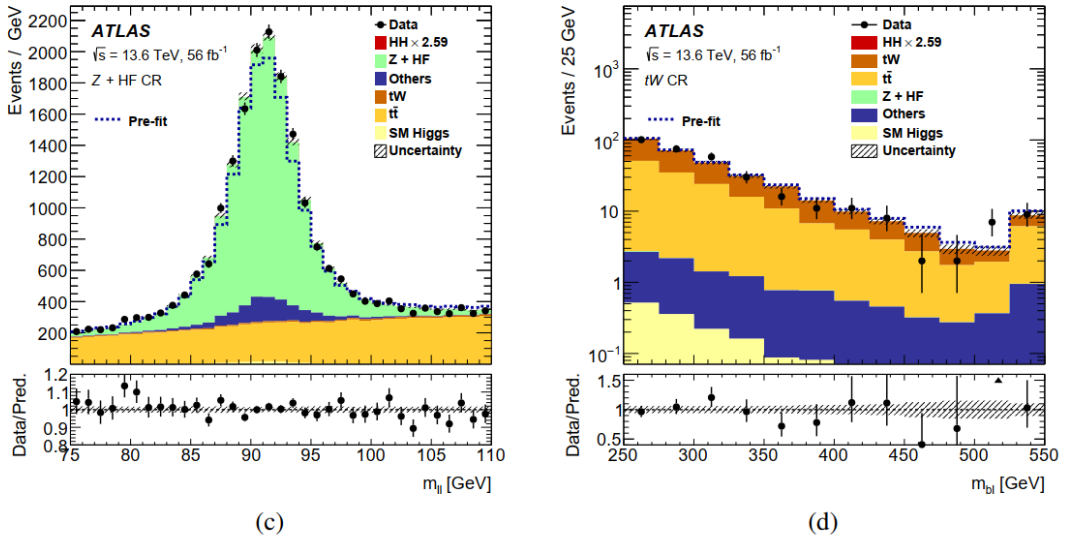
Post-fit results: norm factors and CRs



Run 2



Run 3



Z+hf, $t\bar{t}$ and tW are well constrained by the CRs, which show good post-fit data-to-MC agreement.

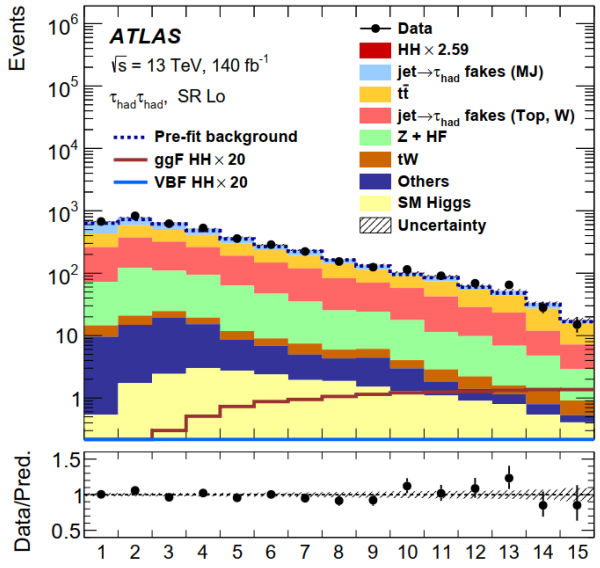
Data/MC: Run 2

ggF low-m_{HH}

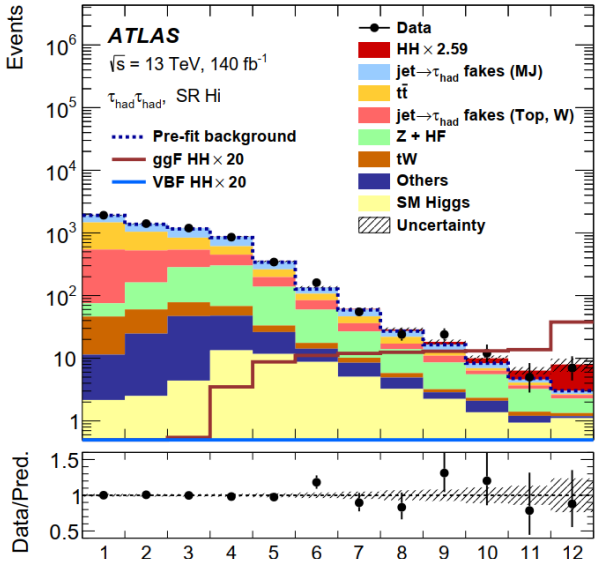
ggF high-m_{HH} drives the sensitivity

VBF

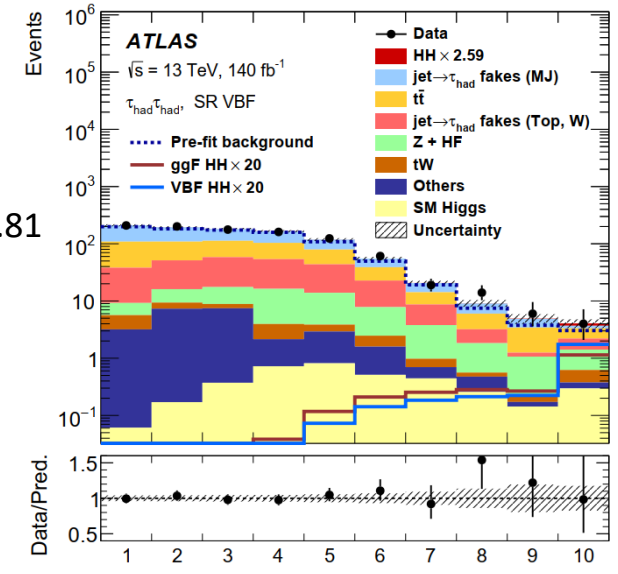
$\tau_{had}\tau_{had}$



p_{χ^2}=0.73

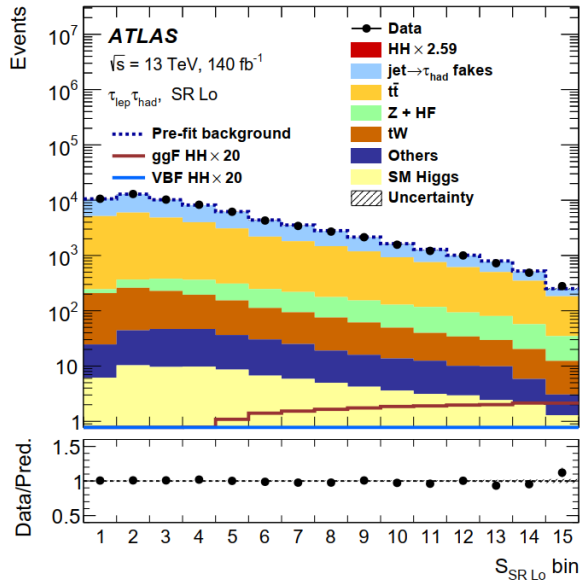


p_{χ^2}=0.81

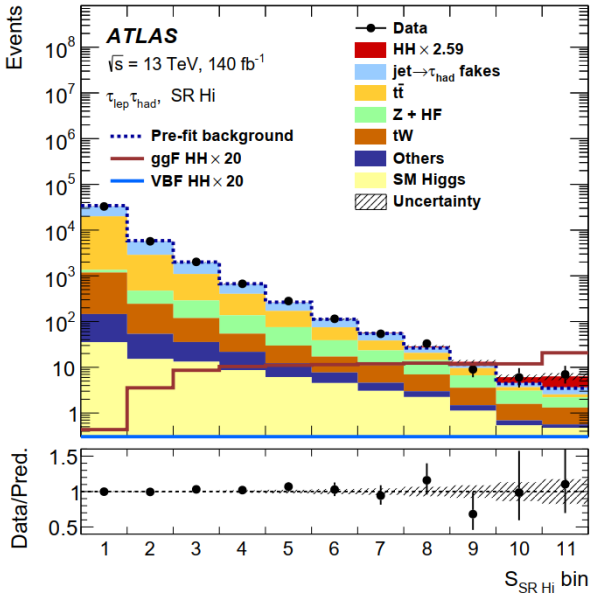


p_{χ^2}=0.98

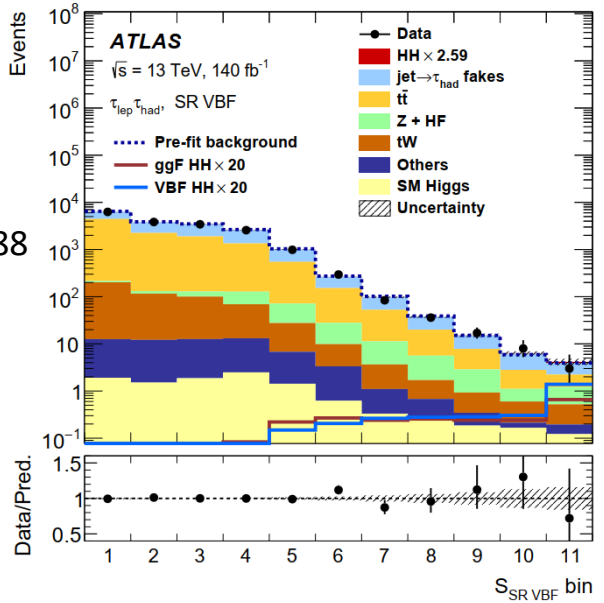
$\tau_{lep}\tau_{had}$



p_{χ^2}=0.20

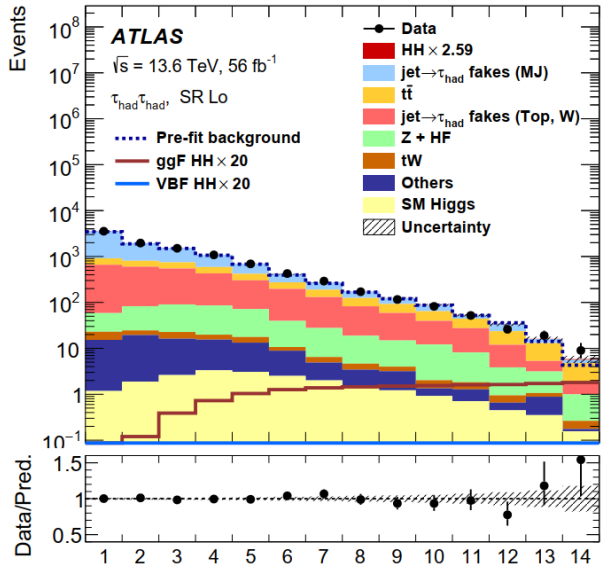
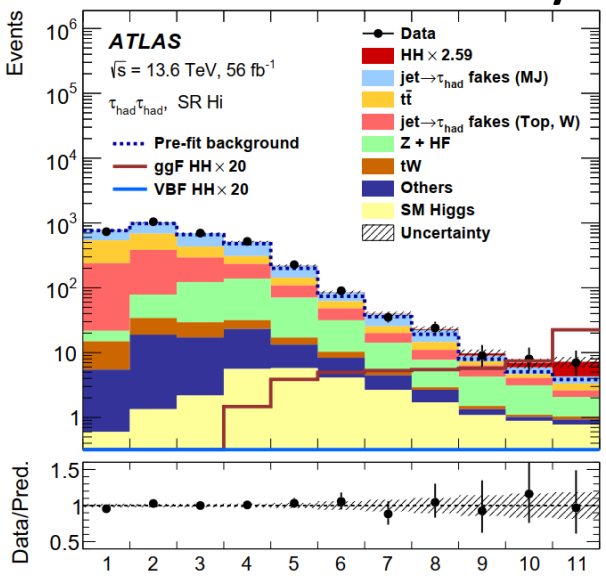
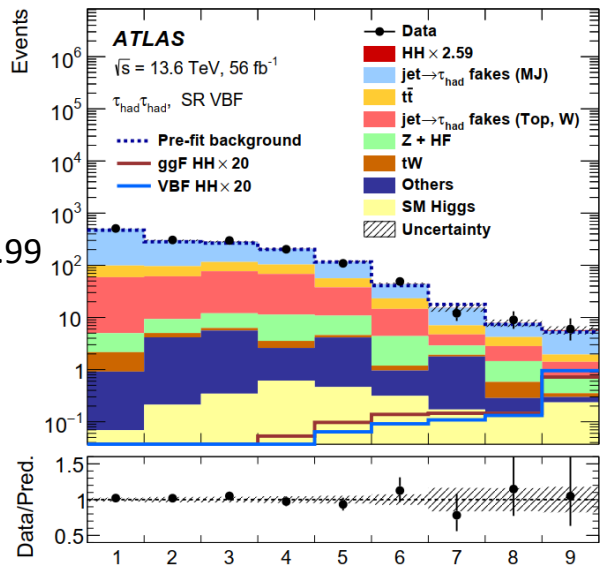
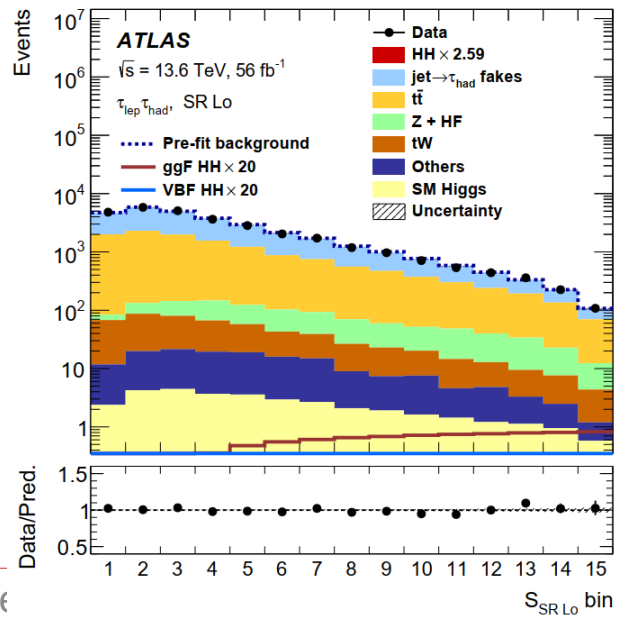
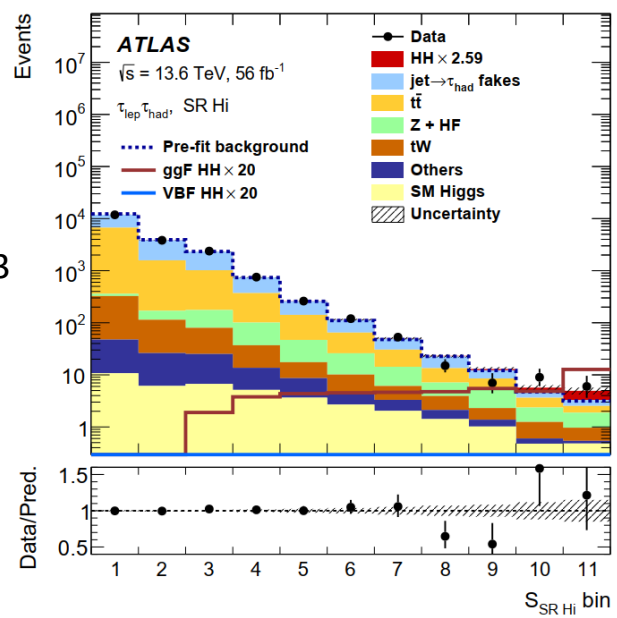
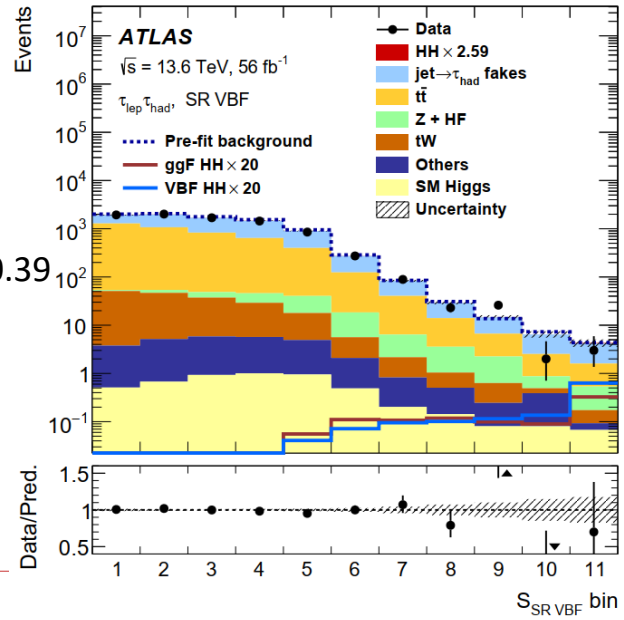


p_{χ^2}=0.88



p_{χ^2}=0.83

Data/MC: Run 3

	ggF low-m_{HH}	ggF high-m_{HH} drives the sensitivity	VBF
$\tau_{had}\tau_{had}$	 p_{χ^2}=0.96	 p_{χ^2}=0.99	 p_{χ^2}=0.97
$\tau_{lep}\tau_{had}$	 p_{χ^2}=0.23	 p_{χ^2}=0.39	 p_{χ^2}=0.09

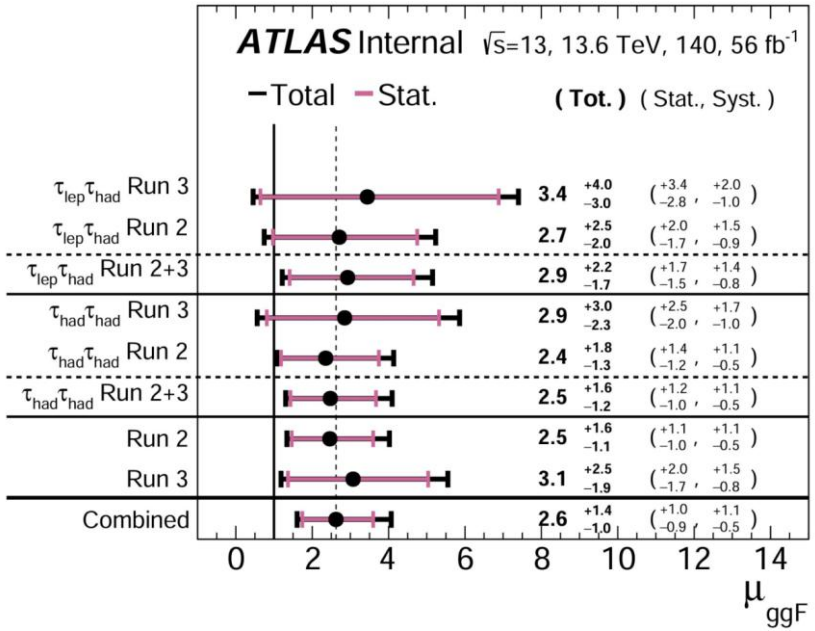
Fit results: $\mu_{\mathrm{ggF}\,HH}$ & $\mu_{\mathrm{VBF}\,HH}$

ggF HH signal strength (fix $\mu_{\mathrm{VBF}\,HH}$=1)

$$\mu_{\mathrm{ggF}\,HH} = 2.6^{+1.4}_{-1.0}$$

Observed (expected) **significance**: 2.64 (1.23)

Observed (expected) **95% CL upper limit**: 5.35 ($1.97^{+0.77}_{-0.55}$ for μ_{HH}=0)

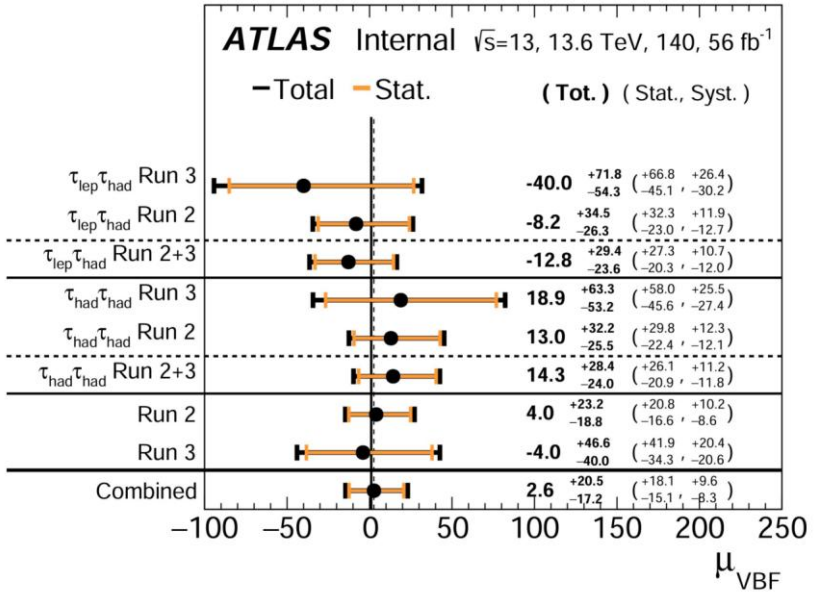


VBF HH signal strength (fix $\mu_{\mathrm{ggF}\,HH}$=1)

$$\mu_{\mathrm{VBF}\,HH} = 2.6^{+20.5}_{-17.2}$$

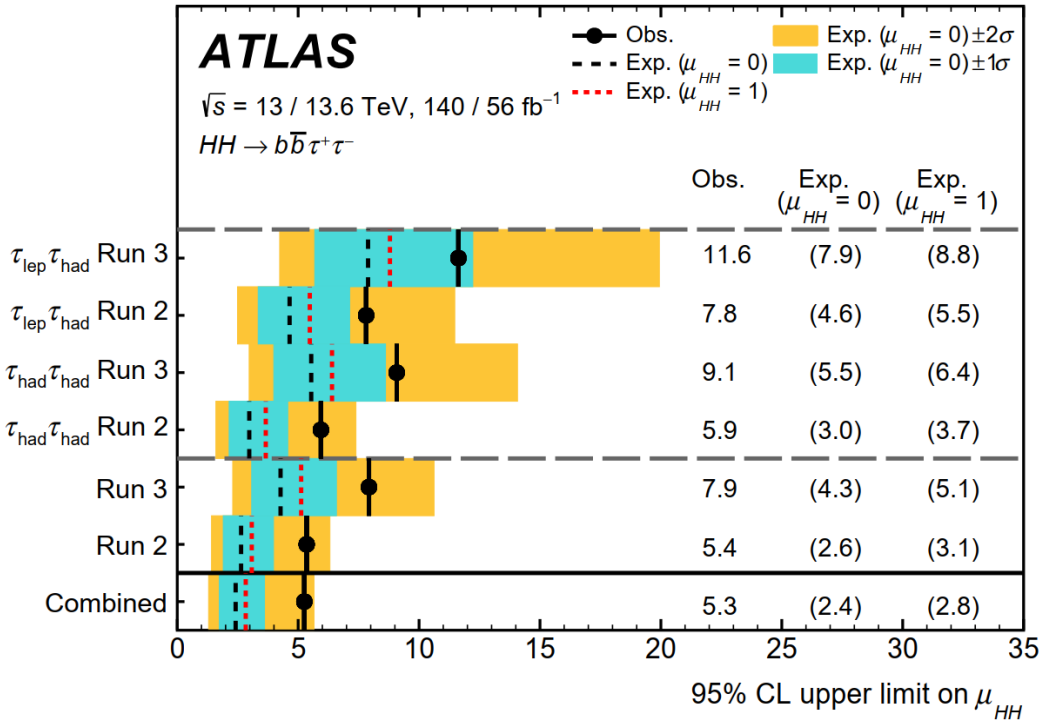
Observed (expected) **significance**: 0.14 (0.06)

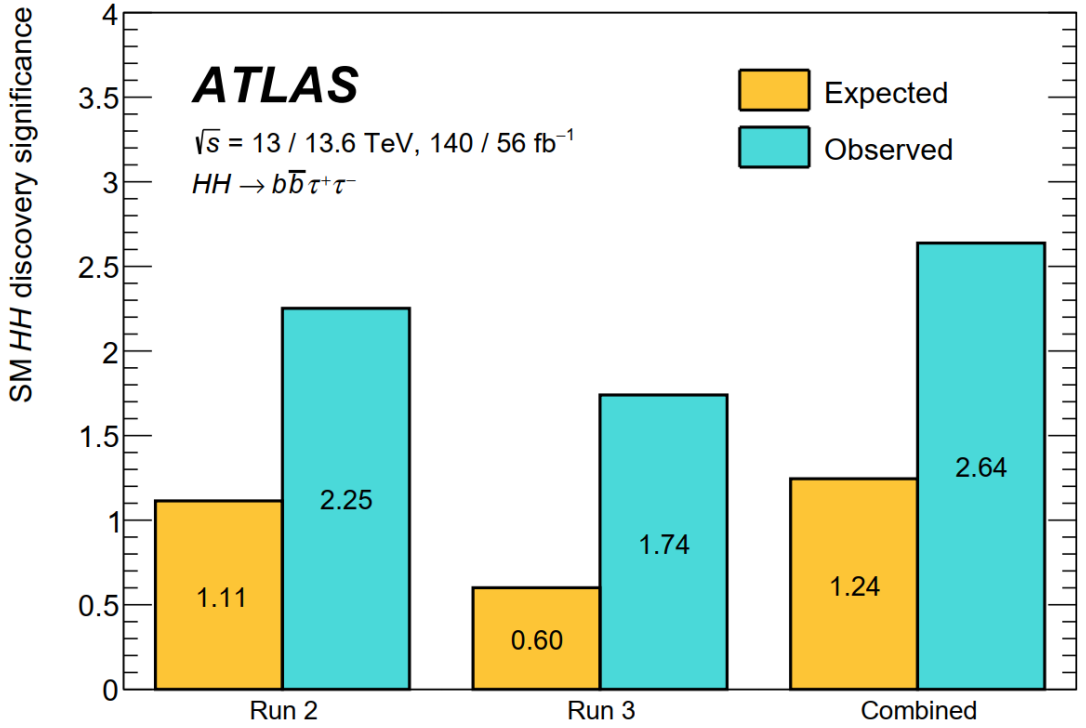
Observed (expected) **95% CL upper limit**: 43.26 ($38.95^{+15.26}_{-10.88}$ for μ_{HH}=0)



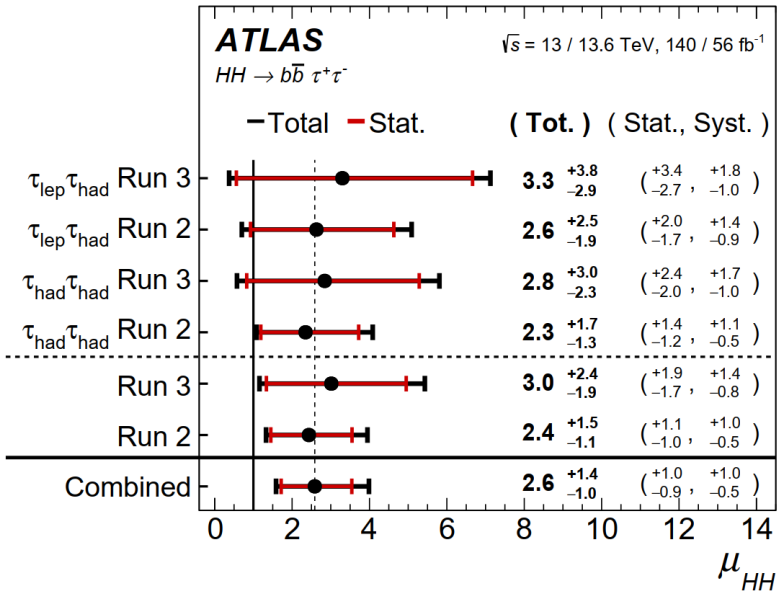
Best-fit μ in individual fit setups

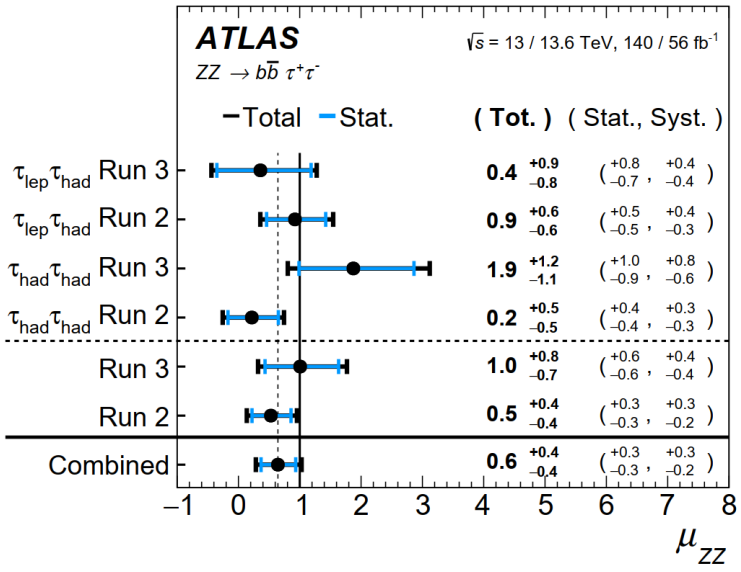
Limit/significance breakdown

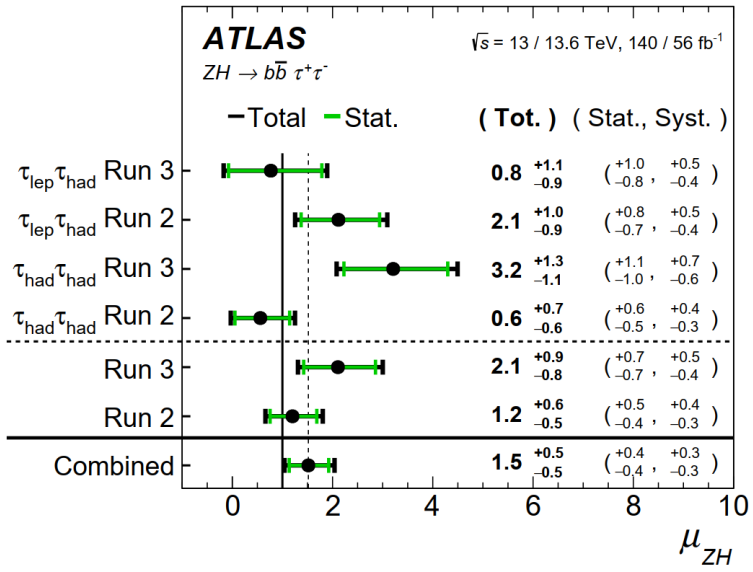




Signal strength







VR distributions

GNN score in two dedicated validation regions (that are overlapping with SR but enriched in bkg):

a) ttbar VR: mMMC >110 GeV and
mMMC + mbb>300 GeV

b) Z VR: mMMC ∈ (70,110) GeV and
$\Delta R(\tau,\tau)$ < (0.06 +0.015·mMMC/GeV)

→ nothing suspicious observed

